Interleukin-33-Activated Islet-Resident Innate Lymphoid Cells Promote Insulin Secretion through Myeloid Cell Retinoic Acid Production

Dalmas, Elise ; Lehmann, Frank M ; Dror, Erez ; Wueest, Stephan ; Thienel, Constanze ; Borsigova, Marcela ; Stawiski, Marc ; Traunecker, Emmanuel ; Lucchini, Fabrizio C ; Dapito, Dianne H ; Kallert, Sandra M ; Guigas, Bruno ; Pattou, Francois ; Kerr-Conte, Julie ; Maechler, Pierre ; Girard, Jean-Philippe ; Konrad, Daniel ; Wolfrum, Christian ; Böni-Schnetzler, Marianne ; Finke, Daniela ; Donath, Marc Y

Abstract: Pancreatic-islet inflammation contributes to the failure of cell insulin secretion during obesity and type 2 diabetes. However, little is known about the nature and function of resident immune cells in this context or in homeostasis. Here we show that interleukin (IL)-33 was produced by islet mesenchymal cells and enhanced by a diabetes milieu (glucose, IL-1 , and palmitate). IL-33 promoted cell function through islet-resident group 2 innate lymphoid cells (ILC2s) that elicited retinoic acid (RA)-producing capacities in macrophages and dendritic cells via the secretion of IL-13 and colony-stimulating factor 2. In turn, local RA signaled to the cells to increase insulin secretion. This IL-33-ILC2 axis was activated after acute cell stress but was defective during chronic obesity. Accordingly, IL-33 injections rescued islet function in obese mice. Our findings provide evidence that an immunometabolic crosstalk between islet-derived IL-33, ILC2s, and myeloid cells fosters insulin secretion.

DOI: https://doi.org/10.1016/j.immuni.2017.10.015

Interleukin-33-Activated Islet-Resident Innate Lymphoid Cells Promote Insulin Secretion Through Myeloid Cell Retinoic Acid Production

Elise Dalmas[1,2,12*], Frank M. Lehmann[2,3], Erez Dror[1,2], Stephan Wueest[4], Constanze Thienel[1,2], , Marcela Borsigova[1,2], Marc Stawiski[1,2], Emmanuel Traunecker[2], Dianne Dapito[5], Fabrizio C. Lucchini[4], Bruno Guigas[6,7], Francois Pattou[8], Julie Kerr-Conte[8], Pierre Maechler[9], Daniel Pinschewer[10], Jean-Philippe Girard[11], Daniel Konrad[4], Christian Wolfrum[5], Marianne Böni-Schnetzler[1,2], Daniela Finke[2,3] and Marc Y. Donath[1,2]

[1]Clinic of Endocrinology, Diabetes and Metabolism University Hospital Basel, 4031 Basel, Switzerland
[2]Department of Biomedicine, University of Basel, 4031 Basel, Switzerland
[3]University of Basel Children's Hospital, 4056 Basel, Switzerland
[4]Department of Pediatric Endocrinology and Diabetology and Children's Research Center, University Children's Hospital, Steinwiesstrasse 75, 8032 Zurich, Switzerland
[5]Institute of Food, Nutrition and Health, ETH-Zürich, Schorenstrasse 16, CH-8603 Schwerzenbach, Switzerland.
[6]Department of Parasitology and Leiden University Medical Center, Leiden, The Netherlands
[7]Department of Molecular Cell Biology, Leiden University Medical Center, Leiden, The Netherlands
[8]University Lille, INSERM, CHU Lille, U1190 Translational Research for Diabetes, European Genomic Institute for Diabetes, EGID, 59000 Lille, France
[9]Department of Cell Physiology and Metabolism & Faculty Diabetes Center, Geneva University Medical Centre, Geneva 4, Switzerland
[10]Division of Experimental Virology, Department of Biomedicine, of Basel, Petersplatz 10, 4009 Basel, Switzerland
[11]Institut de Pharmacologie et de Biologie Structurale, Université de Toulouse, CNRS, UPS, 31077 Toulouse, France
[12]Lead contact
*Correspondence: elise.dalmas@unibas.ch

SUMMARY

Pancreatic islet inflammation contributes to the progression of β cell insulin secretion failure during obesity and type 2 diabetes. However, little is known about the nature and function of resident immune cells in this context and in homeostasis. Here we show that interleukin(IL)-33 is expressed by islet mesenchymal cells and enhanced by a diabetes milieu (high glucose levels, IL-1β and saturated fatty acid). IL-33 promotes β cell function through islet-resident group 2 innate lymphoid cells (ILC2) that elicit retinoic acid (RA)-producing capacities in macrophages and dendritic cells *via* the production of IL-13 and colony-stimulating factor 2. In turn, local RA signals to the β cells to increase insulin secretion. This islet IL-33/ILC2 axis is activated following acute β cell stress but is defective during chronic obesity. Accordingly, injections of IL-33 rescue islet function in obese mice. Our findings provide evidence for a novel immunometabolic crosstalk between islet-derived IL-33, ILC2 and myeloid cells that contributes to the maintenance of insulin secretion.

INTRODUCTION

Type 2 diabetes occurs when pancreatic islet insulin secretion fails to compensate for insulin resistance due to obesity and genetic predisposition. It is now recognized that the immune system plays an important role in these processes and more generally is a regulator of metabolism. Experimental and clinical data have established that white adipose tissue (WAT) is a site of inflammation with ongoing activation of type 1 immunity during obesity-associated metabolic dysfunction (Donath et al., 2013). Interestingly, recent studies suggest a role for resident type 2 immune cells to regulate WAT function and to limit the development of obesity. Indeed, alternatively activated macrophages, regulatory T cells (Tregs), eosinophils and group 2 innate lymphoid cells (ILC2) reside in lean WAT and are altered during obesity (Odegaard and Chawla, 2015). This immunological switch from type 2 to type 1 immunity during obesity is supported by the study of two commonly used mouse strains, C57BL/6 and BALB/c, with marked differences in their immune repertoires (Mills et al., 2000). The Th1-permissive C57BL/6 mice are prone to develop obesity and insulin resistance, while the Th2-permissive BALB/c mice are generally protected against metabolic complications (Montgomery et al., 2013).

During obesity and type 2 diabetes, pancreatic islets also undergo local stress and inflammation, although the etiology and mechanisms differ from adipose tissue. Glucose, saturated fatty acids and bacterial products stimulate islet-derived cytokines such as IL-1β and chemokines that may recruit immune cells (Boni-Schnetzler et al., 2009; Boni-Schnetzler et al., 2008; Maedler et al., 2002). Macrophages are major contributors to islet inflammatory processes (Calderon et al., 2015; Cucak et al., 2014; Eguchi et al., 2012; Ehses et al., 2007; Jourdan et al., 2013; Nackiewicz et al., 2014; Richardson et al., 2009). Accordingly, anti-inflammatory drugs are in development for the treatment of type 2 diabetes (Donath, 2014). However, as in other tissues, islet components of the immune system may have a beneficial role. Indeed, in experimental β cell ablation, alternatively activated macrophages promote β cell proliferation and regeneration, suggesting regulatory

functions of local macrophages (Criscimanna et al., 2014; Nir et al., 2007; Riley et al., 2015; Xiao et al., 2014). It remains unknown whether non-macrophage immune cells also reside in the islets at steady state and contribute to the maintenance of β cell function.

In this study, we sought to identify immune cells residing in pancreatic islets and to investigate their possible role in physiology and disease. By comparing C57BL/6 and BALB/c mice, we identified mesenchymal cell-derived IL-33 as a novel immunoregulatory feature of islets likely to promote β cell function. We show that ILC2 are the primary IL-33-responsive cells in islets, which elicit retinoic acid (RA) production by macrophages and dendritic cells *via* the production of IL-13 and colony stimulating factor 2 (Csf2, also known as GM-CSF). In turn, myeloid cell-derived RA enhances β cell insulin secretion. This novel islet IL-33/ILC2/myeloid cell axis is activated following acute β cell injury but is altered during obesity.

RESULTS

Islet Mesenchymal Cells Produce IL-33

Metabolic comparison of mouse strains showed that intra-peritoneal glucose tolerance tests (GTT) disclosed a more rapid clearance of blood glucose in BALB/c mice compared to age-matched C57BL/6 mice (Figure 1A) with comparable body and adipose mass (Figure S1A). Circulating insulin levels during GTT were similar between the groups (Figure 1B), despite BALB/c mice being more insulin sensitive than C57BL/6 mice (Figure S1B) and similar expression of uncoupling protein 1 (UCP1) in their brown adipose tissue (Figure S1C). These observations point to a stronger insulin secretion in BALB/c mice compared to C57BL/6 mice. Indeed, the insulinogenic index (defined as the ratio of the insulin to glucose areas under the curve) during GTT was higher in BALB/c mice compared to C57BL/6 mice (Figure 1C). To confirm a better β cell function, we tested pancreatic islets *ex-vivo*. Glucose-stimulated insulin secretion (GSIS) was much stronger in BALB/c islets compared to C57BL/6 islets (Figure 1D), with comparable islet insulin content (Figure S1D). We hypothesized that this difference may be due to the BALB/c mouse immune background and measured gene expression of type 2 immune initiators in islets (McKenzie et al., 2014). BALB/c islets showed increased expression of *Il33* but not of *Tslp* (Thymic stromal lymphopoietin) and *Il25* compared to C57BL/6 islets (Figure 1E).

We next employed an *Il33–LacZ gene trap* reporter strain to visualize the activity of the endogenous *Il33* promoter in the pancreas (Pichery et al., 2012). Galactosidase staining revealed constitutive activity of the *Il33* promoter in islets and to a much lesser extent in the exocrine pancreas (located in some vascular beds) of $Il33^{Gt/+}$ mice, with no signal in the pancreas of $Il33^{+/+}$ wildtype (WT) mice (Figure 1F and S1E). To study the cellular origin of IL-33, we sort-purified islet $CD45^{+}$ immune cells and the CD45-negative remaining cells. *Il33* mRNA levels were increased in the $CD45^{-}$ cells compared to the immune compartment (Figure 1G). We next analyzed islets isolated from a green fluorescent protein (GFP) IL-33 reporter mice by flow cytometry (Kallert et al., 2017; Oboki et al., 2010). GFP expression was exclusively detected in cells that were $CD45^{-}$

FSC^{low}SSC^{low} and negative for the Epithelial cell adhesion molecule (Epcam), suggesting a nonepithelial phenotype and thus not related to an endocrine origin (Figure 1H and I). The IL-33-GFP^{+} cells were further classified as positive for the mesodermal stem cell antigen-1 (Sca-1) (Figure 1J) and they preferentially expressed the mesenchymal marker *Vim* (vimentin) and not the smooth muscle cell marker *Acta2* (α-SMA) compared to β cell-enriched and other GFP^{-} subsets (Figure S1F). We confirmed that sort-purified islet Sca-1^{+} cells were the primary population expressing vimentin in islets compared to β cell-enriched and other Sca-1^{-} cells (Figure 1K).

To characterize IL-33 in islets, we stimulated islets with components of a type 2 (obesity-associated) diabetes milieu. High concentrations of recombinant IL-1β, glucose and the saturated fatty acid palmitate induced IL-33 mRNA and protein in C57BL/6 and BALB/c mouse islets relative to controls (Figure 1L and S1G), with BALB/c islets overall producing more IL-33 than C57BL/6 islets. Of note, IL-33 protein was undetectable in islet cell lysate isolated from IL-33-deficient (*Il33*$^{Gt/Gt}$) mice compared to WT controls (Figure S1H). Similar induction of IL-33 was observed in islets isolated from human donors, especially in response to IL-1β (Figure 1M and S1I). Taken together, our results prompted us to investigate a possible role for mesenchymal cell-derived IL-33 as a new islet stress signal regulating endocrine function.

Islet IL-33-Responsive Cells Are Resident Group 2 Innate Lymphoid Cells

Supporting a local role for IL-33, we sought to identify resident IL-33-responsive cells within islets. In contrast to *Il33*, its receptor Interleukin-1 receptor-like 1 (*Il1rl1*, encoding T1/ST2) was more expressed in CD45^{+} cells than in the non-immune cell fraction (Figure 2A). Using flow cytometry, we quantitatively profiled islet-dwelling immune cells of BALB/c and C57BL/6 mice fed a chow diet (gating strategy in Figure S2A). Islets generally contain an average of 6 pan CD45^{+} immune cells per islet, with macrophages being the main immune subset (Figures 2B-C). Interestingly, BALB/c mouse islets showed increased frequency and cell number of specific branches of innate immunity

including ILC2, dendritic cells and NK cells compared to C57BL/6 mice (Figure 2B-C). Islets of both strains contained similar amounts of T and B cells and scarce neutrophils and eosinophils (Figure 2B-C). We identified ILC2 as the primary immune subset expressing IL-33-receptor T1/ST2 within islets (Figure 2D). Rare Tregs were detectable among islet T cells and did not express T1/ST2 (data not shown). Of note, T1/ST2 was also not detectable on the surface of mouse insulin$^+$ β cells (data not shown). Islet-resident ILC2 were lineage negative and expressed the cell surface markers CD90.2, T1/ST2 and KLRG1 and the transcription factor GATA binding protein 3 (GATA3) (Figures 2E and S2A). Islet-resident ILC2 were more frequent among total CD45$^+$ cells (Figure S2B) and expressed higher levels of T1/ST2 (Figure 2F) than ILC2 isolated from the exocrine stroma of the same pancreas, supporting islet ILC2 specificity. Immunofluorescence analyses confirmed the presence of ILC2 located inside the islets (Figure 2G) or in a peri-islet position (Figure S2C) in *Rag2*$^{-/-}$ mouse pancreas. Freshly isolated islets and sort-purified pancreatic ILC2 produced significant amounts of type 2 immune cytokines including IL-5, IL-13 and Csf2 in response to IL-33 and IL-2 *ex vivo* (Figure 2H). ILC3 are also known to produce Csf2 (Mortha et al., 2014). Compared to GATA3$^+$ ILC2, frequencies of RAR-related Orphan Receptor (ROR)γt$^+$ ILC3 were very low in isolated islets and whole pancreata of mice fed a chow diet (Figure 2E and S2D), supporting ILC2 as a major source of Csf2 in islets. We next observed that IL-33-deficient mice exhibited a 42 ± 8 % decrease in ILC2 number in islets compared to WT controls (Figure I). Thus, resident ILC2 are the primary cells that may respond to IL-33 in islets and endogenous IL-33 is required to maintain the islet ILC2 population.

IL-33 Promotes Insulin Secretion

To examine the effects of IL-33 signaling in islet-resident ILC2 *in vivo*, C57BL/6 mice fed a chow diet were administered a single (acute) or three doses (chronic) every other day of saline or mouse recombinant IL-33. IL-33 did not alter body weight and adipose mass (Figure 3A). Acute and chronic IL-33 treatment significantly decreased fasting blood glucose and markedly enhanced

glucose clearance during GTT relative to saline controls (Figure 3B). Interestingly, circulating insulin levels during GTT tended to be boosted following a single injection of IL-33 and reduced upon chronic IL-33 treatment (Figure 3C). Notably, the insulinogenic index was increased upon both acute and chronic IL-33 treatments compared to controls (Figure 3D), pointing to overall increased insulin secretion and progressively enhanced glucose disposal. Supporting this hypothesis, islets isolated from IL-33-treated mice dose-dependently showed enhanced GSIS compared to saline controls (Figure 3E). IL-33-treated mouse islets also had a better insulin secretion relative to controls in response to membrane-depolarizing concentrations of potassium chloride, known to trigger robust secretory response (Figure 3F). Islet insulin content following both GSIS and potassium chloride-induced insulin secretion assays was not different between the groups (Figure S3A and B). Supporting a role for IL-33 to potentiate β cell function and not mass, IL-33 treatment did not alter pancreatic β cell area (Figure G), islet size distribution and islet β cell frequency compared to saline groups (Figures S3C and D). Interestingly, when the three doses of 0.5 μg were administered together in a single injection of 1.5 μg, IL-33 did not significantly improve glucose tolerance and GSIS compared to saline and the usual chronic IL-33-treated groups, arguing for time-dependent improvement of β cell function (Figures S3E and F).

We next investigated whether IL-33 administration improved insulin sensitivity in the peripheral organs. IL-33 did not affect overall insulin sensitivity as demonstrated by both insulin tolerance test (Figure 3H) and hyperinsulinemic-euglycemic clamps (Figure 3I). Accordingly, glucose infusion rate (Figure 3I) and endogenous glucose production (Figure S3G) during clamps were not different between the groups. Tissue glucose uptake was up-regulated in inguinal (Ing)WAT but not in skeletal muscle, epididymal (Epi)WAT and brown adipose tissue (Figure 3J). IngWAT is the most prone to beiging of its white adipocytes, which may contribute to the clearance of blood glucose (Kajimura et al., 2015). Recently, studies have identified a crucial role for IL-33 to elicit WAT beiging and regulate thermogenesis (Brestoff et al., 2015; Lee et al., 2015; Odegaard et al., 2016). Under our conditions, although chronic IL-33 treatment increased *Ucp1* mRNA levels in

EpiWAT (Figure S3H), no change in UCP1 protein was observed in IngWAT of IL-33-treated mice compared to saline groups (data not shown). Importantly, IL-33 treatment still achieved significant improvement in the glucose clearance during GTT in *Ucp1*$^{-/-}$ mice compared to controls (Figure 3K), indicating that recruitment of beige fat is dispensable for the IL-33-induced metabolic effect. We also performed pancreas perfusions to study *in situ* GSIS independently of peripheral glucose consumption. In this experimental setting, chronically IL-33-treated mice tended to have increased insulin secretion compared to saline-treated group (Figure S3I), further supporting IL-33 as an insulin secretagogue.

To investigate endogenous IL-33 role in metabolism, we characterized IL-33-deficient mice under normal conditions. We did not observe any marked difference in body and adipose tissue mass, glucose tolerance and insulin sensitivity in *Il33*$^{Gt/Gt}$ compared to *Il33*$^{+/+}$ littermates when fed a chow diet (Figure S3J-L). However, islets isolated from *Il33*$^{Gt/Gt}$ chow diet mice displayed an impaired insulin secretion compared to WT littermate islets during *ex vivo* GSIS (Figure 3L), without change in insulin content (Figure S3M). Only when challenged with a high fat diet, *Il33*$^{Gt/Gt}$ mice exhibited obesity, glucose intolerance and insulin resistance compared to WT controls (Figure S3N and O). Thus, IL-33 may be a critical regulator of β cell function and mediates rapid glucose-lowering effects by stimulation of insulin secretion.

IL-33-Activated ILC2 Promote Insulin Secretion

IL-33 administration increased the number of CD45^{+} cells and more specifically of ILC2, dendritic cells and eosinophils in islets compared to controls (Figure 4A, S4A and B). While the number and frequency of macrophages were decreased, T and B cell, NK cell and neutrophil populations were not significantly affected (Figure 4A and S4A). We also observed higher mRNA expression of typical ILC2-secreted factors including *Il5* (known to mediate eosinophil activation), *Il13* and *Csf2* in islets isolated from IL-33-treated mice compared to controls (Figure 4B). Down-regulation or no change were observed for gene expression of other type 2 immune genes including *Areg*

(encoding amphiregulin), *Il10* and *Tgfb1* (encoded Transforming growth factor-β) and type 1 cytokines including *Il1beta*, *Ccl2* and *Cxcl1*, while *Il4, Interferon gamma (Ifng) and Il22* were undetectable (Figure S4C).

We next investigated whether IL-33-induced insulin secretion was due to the presence of ILC2. Three doses of saline or IL-33 were administered to BALB/c WT, *Rag2*$^{-/-}$ and ILC2-deficient *Rag2*$^{-/-}$*γc*$^{-/-}$ mice. We observed that IL-33 significantly improved glucose tolerance and *ex vivo* GSIS in WT and *Rag2*$^{-/-}$ mice but not in *Rag2*$^{-/-}$*γc*$^{-/-}$ mice compared to saline (Figure 4C and D), with a slight increase in insulin content in WT and *Rag2*$^{-/-}$ mice (Figure S4D). We next treated *Rag2*$^{-/-}$ mice with an anti-CD90.2 antibody, which is known to deplete ILC2 (Monticelli et al., 2011). Anti-CD90.2-treated mouse islets showed a 58 ± 6% decrease in ILC2 number (Figure 4E) and tended to have impaired GSIS compared to Immunoglobulin G (IgG) controls (Figure 4F), without change in insulin content (Figure S4E).

To further confirm that IL-33 promotes insulin production in an ILC2-dependent manner, *Rag2*$^{-/-}$*γc*$^{-/-}$ mice were treated with IL-33 in the presence or absence of adoptively transferred pancreatic ILC2. ILC2-reconstituted *Rag2*$^{-/-}$*γc*$^{-/-}$ mice supported IL-33-induced ILC2 expansion in their pancreata relative to controls (Figure S4F), without alteration of body and fat mass (Figure S4G). Strikingly, ILC2 transfer was sufficient to rescue IL-33-induced improvement in glucose tolerance test (Figure 4G) and *ex vivo* GSIS (Figure 4H) in *Rag2*$^{-/-}$*γc*$^{-/-}$ mice, with similar circulating insulin levels and islet insulin content (Figure S4H and I).

We next investigated whether ILC2 could have direct effects on β cells to promote insulin production by culturing islets with conditioned media of sort-purified pancreatic ILC2. We found that ILC2-conditioned media significantly improved islet GSIS compared to unconditioned medium controls (Figure 4I), without affecting insulin content (Figure S4J). Collectively, our data indicate that IL-33-induced insulin secretion is not a direct effect of IL-33 on β cells but requires the unique presence of ILC2 and ILC2-secreted factors.

IL-33/ILC2 Axis Elicits Retinoic Acid-Producing Capacities In Islet Myeloid Cells

Islet ILC2 produce cytokines that are known to shape tissue-specific myeloid cell functional identity (Lavin et al., 2015). Notably, IL-13 and Csf2 imprint RA-producing capacities in macrophages and dendritic cells (Mortha et al., 2014; Yokota et al., 2009). We sought to determine whether the IL-33/ILC2 axis also promoted RA production in islet resident myeloid cells. Vitamin A is oxidized by alcohol dehydrogenases to yield retinal. Retinal is then irreversibly converted to RA by aldehyde dehydrogenases (ALDH), the major isoform of which is encoded by *Aldh1a2.* Interestingly, IL-33 administration dose-dependently up-regulated *Aldh1a2* gene expression in islets compared to saline controls (Figure 5A). We sort-purified islet macrophages and dendritic cells from saline- and IL-33-treated mice. Each subset mainly expressed its lineage characteristic gene *Emr1* (encoding F4/80) and *Flt3*, respectively, ensuring their identity (Figure S5A). Both islet macrophages and dendritic cells showed up-regulation of *Aldh1a2* mRNA in IL-33-treated mice compared to controls (Figure 5B). We next measured the relative ALDH activity in islet individual myeloid cells by flow cytometry using a fluorescent substrate for ALDH (Yokota et al., 2009). Islets treated with ALDH inhibitory diethylaminobenzaldehyde was used as a negative control. According to the morphological analysis of islet macrophages, we identified two distinct populations, R1 and R2 (Figure S5B). IL-33 treatment markedly increased ALDH activity in islet R1 macrophages and dendritic cells compared to controls (Figure 5C and D). Although the frequency of granular R2 macrophages was increased in IL-33-treated mice relative to controls (Figure S5C), R2 macrophage ALDH activity was not inhibited by diethylaminobenzaldehyde, pointing to cell autofluorescence (Figure S5D). Enhanced ALDH activity in both R1 macrophages and dendritic cells was observed in islets isolated from *Rag2*$^{-/-}$ mice but not *Rag2*$^{-/-}\gamma c^{-/-}$ mice following IL-33 treatment, suggesting that IL-33-induced myeloid RA production is ILC2-dependent (Figure 5E-F). Interestingly, dendritic cells overall had higher ALDH activity compared to macrophages in both saline- and IL-33-treated mice.

To identify the ILC2-secreted mediators responsible for increased ALDH activity in myeloid cells during IL-33 treatment, we tested the effect of IL-13 and Csf2. We found that these two molecules together up-regulated the gene expression of *Aldh1a2* in sort-purified islet macrophages (Figure 5G) and in bone marrow-derived dendritic cells (Figure 5H) *in vitro*. Of note, recombinant IL-33 did not induce *Aldh1a2* in myeloid cells *in vitro* (data not shown). Islets cultured in presence of ILC2-conditioned media showed increased *Aldh1a2* gene expression compared to control medium, which was hampered in the presence of combined anti-IL-13 and anti-Csf2 neutralizing antibodies (Figure 5I). Besides, islets showed increased *Aldh1a2* gene expression when stimulated with IL-33 and IL-2 *in vitro* compared to controls, suggesting that resident IL-33-responsive ILC2 polarize neighboring myeloid cells (Figure 5J). Accordingly, IL-33-deficient mice displayed reduced ALDH activity in islet resident dendritic cells (Figure 5K) but not macrophages (Figure S5E) compared to WT littermates. Collectively, these data support that IL-33-activated ILC2 imprint islet resident myeloid cells with RA-producing capacities in an IL-13 and Csf2-dependent ways. Interestingly, dendritic cells but not macrophages are dependent on endogenous IL-33 to sustain a physiological level of ALDH activity in islets.

IL-33-Mediated Insulin Secretion Is Dependent On Vitamin A

Our findings prompted us to investigate whether IL-33-induced insulin secretion is dependent on RA signaling. The pharmaceutical form of RA, all-*trans* RA, significantly induced insulin secretion in islets *in vitro,* with a similar insulin content (Figure 6A and S6A). Many RA biological activities are mediated by RA receptors (RARα, RARβ, and RARγ) or retinoic X receptor (RXRα), whose gene expression can be self-induced (Wu et al., 1992). We observed that all-*trans* RA exclusively up-regulated the gene expression of *Rarb* (encoding RARβ) in islets compared to controls (Figure 6B). Accordingly, ILC2-conditioned media failed to increase insulin secretion in islets cultured in presence of the synthetic RARβ receptor antagonist LE135 compared to control, with similar islet insulin content during GSIS (Figure 6C and S6B).

We next conducted a vitamin A deprivation study. To avoid any developmental confounding effects, the diet was started at 6 weeks of age for 10 weeks. Vitamin A deprivation did not induce alterations in body weight nor in insulin sensitivity compared to the control chow diet (Figure S6C and D). Both vitamin A deficient diet- and chow diet-fed mice were chronically treated with three doses of IL-33 or saline. Notably, vitamin A deficiency did not hinder IL-33-mediated activation of ILC2 with similar ILC2 and eosinophil numbers in islets isolated from control and vitamin A deficient mice (Figure 6D). In contrast, IL-33 administration failed to induce *Aldh1a2* gene expression in islets isolated from vitamin A-deprived mice compared to the corresponding chow diet and saline groups (Figure 6E). Reduced ALDH activity was confirmed in islet dendritic cells and to a lesser extent in R1 macrophages isolated from IL-33-treated vitamin A deprived *versus* chow diet mice (Figure S6E). We did not observe any difference in blood glucose and plasma insulin levels during GTT between the groups (Figure S6F). However, the insulinogenic index was significantly increased in IL-33-treated compared to saline-treated chow diet mice but not in vitamin A-deprived mice (Figure 6F), suggesting that IL-33-induced insulin secretion is reduced in the absence of vitamin A. To further investigate the contribution of vitamin A to IL-33-induced insulin effect, we performed *ex vivo* experiments with isolated islets. IL-33 treatment significantly increased insulin secretion during both GSIS and potassium chloride-induced insulin secretion in islets isolated from chow diet but not from vitamin A-deprived mice compared to saline groups (Figure 6G and H), without marked change in insulin content (Figure S6G and H). Therefore, enhancement of β cell function by IL-33 is dependent on dietary vitamin A and its conversion into RA.

Chronic *Versus* Acute Islet Inflammation Regulates The IL-33/ILC2 Axis

To investigate the role of the IL-33/ILC2 axis in a pathophysiological context, mice were fed a chow or high fat diet for 3 to 7 months. At 3 months, obese mice already showed increased body weight and impaired GTT (Figure S7A-B). Notably, obesity was associated with a pathological increase in plasma insulin levels to compensate for insulin resistance and characterized by the

absence of glucose-induced insulin production at 15 min compared to baseline (Figure S7C). Islets isolated from obese mice showed a progressive decrease in *Il33* mRNA levels after 3 and 7 months of high fat diet and in IL-33 protein after 3 months compared to controls (Figure 7A and B). Accordingly, islets isolated from obese mice displayed decreased frequency and number of ILC2 than those isolated from chow diet controls (Figure 7C). This was accompanied by a late decrease in islet *Aldh1a2* gene expression in obese mice relative to controls (Figure 7D). 7 month-obese mice treated with three doses of IL-33 showed a drastic improvement in glucose clearance during GTT (Figure 7E), despite no change in body and WAT weights (Figure S7D). IL-33-treated mice overall lowered their insulin levels but rescued GSIS at 15 min during GTT compared to baseline (Figure 7F). Of note, obesity did not hinder IL-33-mediated type 2 immunity with a significant accumulation of ILC2 and subsequently eosinophils in islets compared to saline controls (Figure S7E).

We next employed a model of acute β cell injury following a single high-dose of streptozotocin, selectively toxic to β cells (Figure S7F). Streptozotocin treatment induced a strong diabetic phenotype characterized by increased fasting blood glucose, decreased fasting circulating insulin levels and body weight loss compared to buffer-treated mice (data not shown). Streptozotocin-treated mice showed increased islet *Il33* mRNA levels compared to controls (Figure 7G) and a more diffuse galactosidase staining in *Il33*$^{Gt/+}$ mice (Figure S7G), pointing towards a more active *Il33* promoter. Accordingly, streptozotocin treatment increased the frequency and number of ILC2 in islets compared to controls (Figure 7H), together with increased islet *Aldh1a2* gene expression (Figure 7I). IL-33 treatment in streptozotocin-induced diabetic mice significantly improved the fasting glycemia and prevented body weight loss compared to controls (Figure 7J), with a tendency towards increased fasting plasma insulin levels on day 9 (Figure S7H) and larger epiWAT (Figure S7I). In contrast, administration of the ILC2-depleting anti-CD90.2 antibody in streptozotocin-induced diabetic *Rag2*$^{-/-}$ mice tended to worsen fasting blood glucose levels compared to IgG controls (Figure 7K). We did not detect any difference in glycemia when *Il33*$^{Gt/Gt}$

and WT littermates were treated with a similar streptozotocin high dose (data not shown). Taken together, our results show that the IL-33/ILC2 axis is defective in islets during obesity and is activated following acute β cell stress. ILC2 may not only boost insulin secretion but also contribute to β cell recovery following injury.

DISCUSSION

Our work established a role for type 2 immunity in the regulation of pancreatic islet physiology orchestrated by IL-33. Many studies described IL-33 expression in mouse tissues at steady state, including in epithelial cells of barrier tissues, fibroblast-like cells in lymphoid organs or endothelial cells in adipose tissue (Liew et al., 2016). In patients suffering from chronic pancreatitis, IL-33 was mainly expressed by activated pancreatic stellate cells (Masamune et al., 2010). Here, using two different models of IL-33 reporter mice, we identified IL-33-producing cells as Sca-1^{+}vimentin^{+} mesenchymal cells located inside pancreatic islets. In mouse and human islets, IL-33 gene expression and protein levels were increased upon stimulation with components of a diabetic milieu, proposing IL-33 as a novel stress signal in islets. Indeed, designated as an « alarmin », IL-33 is usually released after cell injury to alert the immune system and initiate repair processes (Liew et al., 2016). We detected IL-33 protein only in islet cell lysate and not in the supernatant. This argues in favor of IL-33 nuclear localization and the requirement for cell death for its proper release. Alternatively, detection of IL-33 in islet cell supernatant may be hindered by its low concentration and rapid inactivation in the extracellular environment through caspase-mediated cleavage and oxidation of cysteine residues (Liew et al., 2016). Although the role of islet mesenchymal cells remains to be explored, we showed that IL-33 promotes and sustains β cell function in chow diet-fed mice. Indeed, administration of a single or three doses of IL-33 significantly stimulated insulin secretion. In severely obese mice, IL-33 injections rescued GSIS during GTT relative to controls. Conversely, islets isolated from IL-33-deficient mice displayed impaired GSIS compared to WT littermates. Supporting our findings, mice lacking IL-33 receptor T1/ST2 develop hyperglycemia associated with impaired insulin secretion when fed a high fat diet (Miller et al., 2010). In contrast to published data linking IL-33 deficiency to obesity, glucose intolerance (Brestoff et al., 2015) and thermogenesis defect (Odegaard et al., 2016), we did not detect any other metabolic alterations in chow diet-fed *Il33*$^{Gt/Gt}$ knockout mice relative to WT

littermates. These divergent findings may arise from variations in dietary fat and sucrose content and the use in our study of littermate controls backcrossed on a pure genetic background.

Growing emphasis was laid on the protective role of IL-33 in obesity. This effect has been widely attributed to IL-33-induced modulation of WAT inflammation towards type 2 immunity that may promote insulin sensitivity (Kolodin et al., 2015; Miller et al., 2010; Molofsky et al., 2013; Molofsky et al., 2015; Vasanthakumar et al., 2015). In genetically or diet-induced obese mice, IL-33 treatment led to an improvement in glucose homeostasis compared to controls. However, this phenotype was not associated with enhanced insulin sensitivity (Miller et al., 2010; Vasanthakumar et al., 2015). Here, we also showed that IL-33 treatment improves glucose tolerance in chow diet mice independently of insulin sensitivity. Recently, IL-33 was shown to elicit WAT beiging and to regulate the splicing of *Ucp1* mRNA (Brestoff et al., 2015; Lee et al., 2015; Odegaard et al., 2016). It is now recognized that beige adipose cells have the capacity to consume glucose to produce heat (Kajimura et al., 2015). While glucose uptake was increased in ingWAT of IL-33-treated mice, chronic IL-33 treatment failed to induce UCP1 protein in WAT compared to controls, suggesting that our experimental settings are not yet sufficient to stimulate the growth of functional beige fat. Indeed, publications reporting IL-33-mediated beiging were based on daily IL-33 injections for more than a week (Brestoff et al., 2015; Lee et al., 2015). Importantly, treatment of *Ucp1*-deficient mice confirmed that IL-33 metabolic effects do not rely on recruitment of beige adipocytes to clear the blood glucose. Thus, IL-33 treatment in chow diet-fed mice mainly lowers glycemia by rapid stimulation of insulin secretion in β cells, independently of changes in both insulin sensitivity and adipose beiging. The fact that IL-33 treatment tends to lower plasma insulin levels during GTT may be in response to alternative IL-33 glucose-lowering effects, including glucose consumption by increased number of activated immune cells compared to controls.

IL-33 signals through the T1/ST2 receptor identified on the surface of many immune cells.

Although IL-33 was shown to induce oxidative stress in the MIN6 insulinoma β cell line (Hasnain et al., 2014), we did not detect T1/ST2 on the surface of mouse islet β cells but on resident immune cells. In contrast to autoimmune type 1 diabetic mouse models, there are only a limited number of studies addressing the nature of islet immune cells in WT mice at steady state or in the context of type 2 diabetes. Besides, the different protocols used to isolate islets and disperse them into single cells may affect immune cell purity, number and surface markers. Likewise, the amount of islets (from one or several pooled mice) used for immune profiling may greatly influence the outcomes considering that immune cells represent only a small fraction of islet cells, that we and others have estimated to range from 2 to 10 immune cells per islet (Calderon et al., 2015; Calderon et al., 2008; Cucak et al., 2014; Ehses et al., 2007). In our study, we used clean handpicked islets that were isolated from pools of mice. We confirmed that macrophages are the major immune cell population existing within islets of chow diet mice (Calderon et al., 2015; Cucak et al., 2014). Yet we also noticed cells from the non-macrophage compartment including ILC2, dendritic cells and NK cells that were more abundant in BALB/c mice compared to C57BL/6 mice. Among them, we identified resident ILC2 as the primary islet IL-33-responsive cells, which were located inside and in the periphery of islets, likely to influence β cell function.

ILC2 are rare yet potent tissue-resident cells under physiological conditions (Gasteiger et al., 2015). Emerging studies have extended their biological functions to immunosurveillance, tissue protection, repair processes and now adipose beiging (Brestoff et al., 2015; Lee et al., 2015; McKenzie et al., 2014). Our work provides further evidence on how these cells regulate the host metabolism by identifying a novel ILC2 metabolic function in islets. IL-33 treatment in *Rag2*$^{-/-}$ mice, *Rag2*$^{-/-}$*γc*$^{-/-}$ mice and ILC2-adoptively transferred *Rag2*$^{-/-}$*γc*$^{-/-}$ mice confirmed that IL-33 does not act directly on β cells but is dependent on the presence of ILC2 and ILC2-secreted factors to promote insulin secretion. IL-33 administration led to a massive accumulation of ILC2 and

subsequently dendritic cells and eosinophils. Thus, we cannot rule out a possible role for eosinophils in IL-33-mediated metabolic benefits. The IL-33/ILC2 axis also contributes to β cell protection in the context of obesity- and streptozotocin-induced β cell stress, supporting its functional role. Similar to adipose tissue (Molofsky et al., 2013), obesity is associated with a loss of islet ILC2. This may partly be explained by the phenotypic plasticity that ILC2 exhibit in response to inflammatory cues including IL-1β (Ohne et al., 2016), known to be elevated during obesity and type 2 diabetes in islets (Donath et al., 2013).

Islet ILC2 produced IL-13 and Csf2 that are recognized to induce RA-producing capacities in myeloid cells (Mortha et al., 2014; Yokota et al., 2009). Here, we show that approximately 30% of resident dendritic cells and 5% of macrophages displayed ALDH activity in islets under physiological conditions. These RA-producing capacities are markedly increased after IL-33 treatment compared to saline groups but diminished (for dendritic cells) in IL-33-deficient mice compared to WT mice. We propose that ILC2-derived IL-13 and Csf2 may be the mediators promoting ALDH activity in islet myeloid cells. Recently, a similar crosstalk was described in the mouse intestine. Microbiota-driven IL-1β production by macrophages promotes the release of Csf2 by RORγt^{+}ILC3, which in turn regulates RA production in phagocytes and leads to local Treg homeostasis (Mortha et al., 2014). Our study reveals that mesenchymal cell-derived IL-33 initiates an immune crosstalk between islet ILC2 and neighboring myeloid cells to produce RA and promote insulin secretion, not related to classical immune responses.

Previous studies have established that vitamin A and its metabolite RA play a crucial role in the maintenance of pancreatic endocrine functions. Vitamin A-deficient diet or RA-related gene deficiencies blocked the development of fetal pancreatic islets and abrogates the maintenance of β cell mass and function during adulthood (Brun et al., 2015; Chertow et al., 1987; Martin et al.,

2005; Matthews et al., 2004; Perez et al., 2013; Trasino et al., 2016). However the cellular source of RA in islets in adult mice remained elusive. Our data identified islet resident macrophages and especially dendritic cells as endogenous RA producers. We used a vitamin A-deficient diet that was given to 6-week-old adult mice to avoid any developmental issues. In contradiction to published data (Trasino et al., 2016), vitamin A-deprived mice did not show impaired glucose homeostasis *per se.* However, we observed that IL-33 treatment did not promote β cell function in vitamin A-deprived mice in contrast to IL-33 treatment in control mice, supporting that IL-33-induced insulin secretion requires vitamin A and its conversion to RA.

In summary, our study identifies the first immunometabolic crosstalk within islets that is initiated by IL-33-releasing mesenchymal cells and leads to a novel insulin secretagogue effect. IL-33 acts on resident ILC2 that elicit RA-producing capacities in myeloid cells to support insulin secretion. This work represents an important step towards our understanding of islet resident immune cells and show that ILC2 can influence β cell physiology. In addition to blocking pro-inflammatory type 1 immunity, selective activation of type 2 immunity *via* IL-33 or ILC2 stimulation may offer therapeutic avenues for novel immunotherapies in patients suffering from type 2 diabetes. Indeed, targeting the IL-33/ILC2 pathway in obesity appears optimal as it promotes both rapid insulin secretion and long-term adipose beiging development, without affecting insulin sensitivity and thus further risk of body weight gain.

AUTHOR CONTRIBUTIONS

E.Da. and M.Y.D. conceived the project and wrote the manuscript; E.Da. performed and analyzed the experiments; F.M.L. performed pancreatic ILC2 sorting, BM-DCs and ILC2 immunofluorescence; E.Dr., C.T., M.Bor., M. S., M.Böni. and B.G. helped with experiments; E.T. helped with FACS analyses and cell sorting; S.W., F.C.L. and D.K. performed clamp studies; F.P. and J.K.C. provided human islets; P.M. performed pancreatic perfusions; J-P.G. provided *Il33*$^{Gt/Gt}$ mice; D.Pi. provided *Il33*$^{gfp/wt}$ mice; D.Pa. and C.W. performed GTT on *Ucp1*$^{-/-}$ mice; D.F. provided expertise, reagents and mice; all co-authors helped with the manuscript.

ACKNOWLEDGMENTS

We are grateful to our technicians Kaethi Dembinski and Stéphanie Häuselmann for their excellent technical assistance; Angela Bosch for performing intravenous injections; Nicole von Burg for her help with BM-DC experiments; Friederike Schulze, Shuyang Traub and Katharina Timper for their comments; and the Flow cytometry, Microscopy and Animal facilities of the Department of Biomedicine (University of Basel). E.Da. was financially supported by the University of Basel Research Fund for Young Researcher and the European foundation for the Study of Diabetes (EFSD)/Lilly Research Fellowship. The study was supported by the Swiss National Science Foundation to M.Y.D. and D.F.

SUPPLEMENTAL INFORMATION

Supplemental Information includes seven figures.

REFERENCES

Boni-Schnetzler, M., Boller, S., Debray, S., Bouzakri, K., Meier, D.T., Prazak, R., Kerr-Conte, J., Pattou, F., Ehses, J.A., Schuit, F.C., and Donath, M.Y. (2009). Free fatty acids induce a proinflammatory response in islets via the abundantly expressed interleukin-1 receptor I. Endocrinology *150*, 5218-5229.

Boni-Schnetzler, M., Thorne, J., Parnaud, G., Marselli, L., Ehses, J.A., Kerr-Conte, J., Pattou, F., Halban, P.A., Weir, G.C., and Donath, M.Y. (2008). Increased interleukin (IL)-1beta messenger ribonucleic acid expression in beta -cells of individuals with type 2 diabetes and regulation of IL-1beta in human islets by glucose and autostimulation. J Clin Endocrinol Metab *93*, 4065-4074.

Brasel, K., De Smedt, T., Smith, J.L., and Maliszewski, C.R. (2000). Generation of murine dendritic cells from flt3-ligand-supplemented bone marrow cultures. Blood *96*, 3029-3039.

Brestoff, J.R., Kim, B.S., Saenz, S.A., Stine, R.R., Monticelli, L.A., Sonnenberg, G.F., Thome, J.J., Farber, D.L., Lutfy, K., Seale, P., and Artis, D. (2015). Group 2 innate lymphoid cells promote beiging of white adipose tissue and limit obesity. Nature *519*, 242-246.

Brun, P.J., Grijalva, A., Rausch, R., Watson, E., Yuen, J.J., Das, B.C., Shudo, K., Kagechika, H., Leibel, R.L., and Blaner, W.S. (2015). Retinoic acid receptor signaling is required to maintain glucose-stimulated insulin secretion and beta-cell mass. FASEB J *29*, 671-683.

Calderon, B., Carrero, J.A., Ferris, S.T., Sojka, D.K., Moore, L., Epelman, S., Murphy, K.M., Yokoyama, W.M., Randolph, G.J., and Unanue, E.R. (2015). The pancreas anatomy conditions the origin and properties of resident macrophages. J Exp Med *212*, 1497-1512.

Calderon, B., Suri, A., Miller, M.J., and Unanue, E.R. (2008). Dendritic cells in islets of Langerhans constitutively present beta cell-derived peptides bound to their class II MHC molecules. Proc Natl Acad Sci U S A *105*, 6121-6126.

Chertow, B.S., Blaner, W.S., Baranetsky, N.G., Sivitz, W.I., Cordle, M.B., Thompson, D., and Meda, P. (1987). Effects of vitamin A deficiency and repletion on rat insulin secretion in vivo and in vitro from isolated islets. J Clin Invest *79*, 163-169.

Criscimanna, A., Coudriet, G.M., Gittes, G.K., Piganelli, J.D., and Esni, F. (2014). Activated macrophages create lineage-specific microenvironments for pancreatic acinar- and beta-cell regeneration in mice. Gastroenterology *147*, 1106-1118 e1111.

Cucak, H., Grunnet, L.G., and Rosendahl, A. (2014). Accumulation of M1-like macrophages in type 2 diabetic islets is followed by a systemic shift in macrophage polarization. J Leukoc Biol *95*, 149-160.

Donath, M.Y. (2014). Targeting inflammation in the treatment of type 2 diabetes: time to start. Nat Rev Drug Discov *13*, 465-476.

Donath, M.Y., Dalmas, E., Sauter, N.S., and Boni-Schnetzler, M. (2013). Inflammation in obesity and diabetes: islet dysfunction and therapeutic opportunity. Cell Metab *17*, 860-872.

Eguchi, K., Manabe, I., Oishi-Tanaka, Y., Ohsugi, M., Kono, N., Ogata, F., Yagi, N., Ohto, U., Kimoto, M., Miyake, K.*, et al.* (2012). Saturated fatty acid and TLR signaling link beta cell dysfunction and islet inflammation. Cell Metab *15*, 518-533.

Ehses, J.A., Perren, A., Eppler, E., Ribaux, P., Pospisilik, J.A., Maor-Cahn, R., Gueripel, X., Ellingsgaard, H., Schneider, M.K., Biollaz, G.*, et al.* (2007). Increased number of islet-associated macrophages in type 2 diabetes. Diabetes *56*, 2356-2370.

Gasteiger, G., Fan, X., Dikiy, S., Lee, S.Y., and Rudensky, A.Y. (2015). Tissue residency of innate lymphoid cells in lymphoid and nonlymphoid organs. Science *350*, 981-985.

Hasnain, S.Z., Borg, D.J., Harcourt, B.E., Tong, H., Sheng, Y.H., Ng, C.P., Das, I., Wang, R., Chen, A.C., Loudovaris, T.*, et al.* (2014). Glycemic control in diabetes is restored by therapeutic manipulation of cytokines that regulate beta cell stress. Nat Med *20*, 1417-1426.

Jourdan, T., Godlewski, G., Cinar, R., Bertola, A., Szanda, G., Liu, J., Tam, J., Han, T., Mukhopadhyay, B., Skarulis, M.C.*, et al.* (2013). Activation of the Nlrp3 inflammasome in infiltrating macrophages by endocannabinoids mediates beta cell loss in type 2 diabetes. Nat Med *19*, 1132-1140.

Kajimura, S., Spiegelman, B.M., and Seale, P. (2015). Brown and Beige Fat: Physiological Roles beyond Heat Generation. Cell Metab *22*, 546-559.

Kallert, S.M., Darbre, S., Bonilla, W.V., Kreutzfeldt, M., Page, N., Muller, P., Kreuzaler, M., Lu, M., Favre, S., Kreppel, F.*, et al.* (2017). Replicating viral vector platform exploits alarmin signals for potent CD8+ T cell-mediated tumour immunotherapy. Nat Commun *8*, 15327.

Kolodin, D., van Panhuys, N., Li, C., Magnuson, A.M., Cipolletta, D., Miller, C.M., Wagers, A., Germain, R.N., Benoist, C., and Mathis, D. (2015). Antigen- and cytokine-driven accumulation of regulatory T cells in visceral adipose tissue of lean mice. Cell Metab *21*, 543-557.

Lavin, Y., Mortha, A., Rahman, A., and Merad, M. (2015). Regulation of macrophage development and function in peripheral tissues. Nat Rev Immunol *15*, 731-744.

Lee, M.W., Odegaard, J.I., Mukundan, L., Qiu, Y., Molofsky, A.B., Nussbaum, J.C., Yun, K., Locksley, R.M., and Chawla, A. (2015). Activated type 2 innate lymphoid cells regulate beige fat biogenesis. Cell *160*, 74-87.

Liew, F.Y., Girard, J.P., and Turnquist, H.R. (2016). Interleukin-33 in health and disease. Nat Rev Immunol *16*, 676-689.

Maechler, P., Gjinovci, A., and Wollheim, C.B. (2002). Implication of glutamate in the kinetics of insulin secretion in rat and mouse perfused pancreas. Diabetes *51 Suppl 1*, S99-102.

Maedler, K., Sergeev, P., Ris, F., Oberholzer, J., Joller-Jemelka, H.I., Spinas, G.A., Kaiser, N., Halban, P.A., and Donath, M.Y. (2002). Glucose-induced beta cell production of IL-1beta contributes to glucotoxicity in human pancreatic islets. J Clin Invest *110*, 851-860.

Martin, M., Gallego-Llamas, J., Ribes, V., Kedinger, M., Niederreither, K., Chambon, P., Dolle, P., and Gradwohl, G. (2005). Dorsal pancreas agenesis in retinoic acid-deficient Raldh2 mutant mice. Dev Biol *284*, 399-411.

Masamune, A., Watanabe, T., Kikuta, K., Satoh, K., Kanno, A., and Shimosegawa, T. (2010). Nuclear expression of interleukin-33 in pancreatic stellate cells. Am J Physiol Gastrointest Liver Physiol *299*, G821-832.

Matthews, K.A., Rhoten, W.B., Driscoll, H.K., and Chertow, B.S. (2004). Vitamin A deficiency impairs fetal islet development and causes subsequent glucose intolerance in adult rats. J Nutr *134*, 1958-1963.

McKenzie, A.N., Spits, H., and Eberl, G. (2014). Innate lymphoid cells in inflammation and immunity. Immunity *41*, 366-374.

Miller, A.M., Asquith, D.L., Hueber, A.J., Anderson, L.A., Holmes, W.M., McKenzie, A.N., Xu, D., Sattar, N., McInnes, I.B., and Liew, F.Y. (2010). Interleukin-33 induces protective effects in adipose tissue inflammation during obesity in mice. Circ Res *107*, 650-658.

Mills, C.D., Kincaid, K., Alt, J.M., Heilman, M.J., and Hill, A.M. (2000). M-1/M-2 macrophages and the Th1/Th2 paradigm. J Immunol *164*, 6166-6173.

Molofsky, A.B., Nussbaum, J.C., Liang, H.E., Van Dyken, S.J., Cheng, L.E., Mohapatra, A., Chawla, A., and Locksley, R.M. (2013). Innate lymphoid type 2 cells sustain visceral adipose tissue eosinophils and alternatively activated macrophages. J Exp Med *210*, 535-549.

Molofsky, A.B., Van Gool, F., Liang, H.E., Van Dyken, S.J., Nussbaum, J.C., Lee, J., Bluestone, J.A., and Locksley, R.M. (2015). Interleukin-33 and Interferon-gamma Counter-Regulate Group 2 Innate Lymphoid Cell Activation during Immune Perturbation. Immunity *43*, 161-174.

Montgomery, M.K., Hallahan, N.L., Brown, S.H., Liu, M., Mitchell, T.W., Cooney, G.J., and Turner, N. (2013). Mouse strain-dependent variation in obesity and glucose homeostasis in response to high-fat feeding. Diabetologia *56*, 1129-1139.

Monticelli, L.A., Sonnenberg, G.F., Abt, M.C., Alenghat, T., Ziegler, C.G., Doering, T.A., Angelosanto, J.M., Laidlaw, B.J., Yang, C.Y., Sathaliyawala, T.*, et al.* (2011). Innate lymphoid cells promote lung-tissue homeostasis after infection with influenza virus. Nat Immunol *12*, 1045-1054.

Mortha, A., Chudnovskiy, A., Hashimoto, D., Bogunovic, M., Spencer, S.P., Belkaid, Y., and Merad, M. (2014). Microbiota-dependent crosstalk between macrophages and ILC3 promotes intestinal homeostasis. Science *343*, 1249288.

Nackiewicz, D., Dan, M., He, W., Kim, R., Salmi, A., Rutti, S., Westwell-Roper, C., Cunningham, A., Speck, M., Schuster-Klein, C.*, et al.* (2014). TLR2/6 and TLR4-activated macrophages contribute to islet inflammation and impair beta cell insulin gene expression via IL-1 and IL-6. Diabetologia *57*, 1645-1654.

Nir, T., Melton, D.A., and Dor, Y. (2007). Recovery from diabetes in mice by beta cell regeneration. J Clin Invest *117*, 2553-2561.

Oboki, K., Ohno, T., Kajiwara, N., Arae, K., Morita, H., Ishii, A., Nambu, A., Abe, T., Kiyonari, H., Matsumoto, K.*, et al.* (2010). IL-33 is a crucial amplifier of innate rather than acquired immunity. Proc Natl Acad Sci U S A *107*, 18581-18586.

Odegaard, J.I., and Chawla, A. (2015). Type 2 responses at the interface between immunity and fat metabolism. Current opinion in immunology *36*, 67-72.

Odegaard, J.I., Lee, M.W., Sogawa, Y., Bertholet, A.M., Locksley, R.M., Weinberg, D.E., Kirichok, Y., Deo, R.C., and Chawla, A. (2016). Perinatal Licensing of Thermogenesis by IL-33 and ST2. Cell *166*, 841-854.

Ohne, Y., Silver, J.S., Thompson-Snipes, L., Collet, M.A., Blanck, J.P., Cantarel, B.L., Copenhaver, A.M., Humbles, A.A., and Liu, Y.J. (2016). IL-1 is a critical regulator of group 2 innate lymphoid cell function and plasticity. Nat Immunol *17*, 646-655.

Perez, R.J., Benoit, Y.D., and Gudas, L.J. (2013). Deletion of retinoic acid receptor beta (RARbeta) impairs pancreatic endocrine differentiation. Exp Cell Res *319*, 2196-2204.

Pichery, M., Mirey, E., Mercier, P., Lefrancais, E., Dujardin, A., Ortega, N., and Girard, J.P. (2012). Endogenous IL-33 is highly expressed in mouse epithelial barrier tissues, lymphoid organs, brain, embryos, and inflamed tissues: in situ analysis using a novel Il-33-LacZ gene trap reporter strain. J Immunol *188*, 3488-3495.

Richardson, S.J., Willcox, A., Bone, A.J., Foulis, A.K., and Morgan, N.G. (2009). Islet-associated macrophages in type 2 diabetes. Diabetologia *52*, 1686-1688.

Riley, K.G., Pasek, R.C., Maulis, M.F., Dunn, J.C., Bolus, W.R., Kendall, P.L., Hasty, A.H., and Gannon, M. (2015). Macrophages are essential for CTGF-mediated adult beta-cell proliferation after injury. Mol Metab *4*, 584-591.

Trasino, S.E., Tang, X.H., Jessurun, J., and Gudas, L.J. (2016). Retinoic acid receptor beta2 agonists restore glycaemic control in diabetes and reduce steatosis. Diabetes Obes Metab *18*, 142-151.

Vasanthakumar, A., Moro, K., Xin, A., Liao, Y., Gloury, R., Kawamoto, S., Fagarasan, S., Mielke, L.A., Afshar-Sterle, S., Masters, S.L.*, et al.* (2015). The transcriptional regulators IRF4, BATF and IL-33 orchestrate development and maintenance of adipose tissue-resident regulatory T cells. Nat Immunol *16*, 276-285.

Wu, T.C., Wang, L., and Wan, Y.J. (1992). Retinoic acid regulates gene expression of retinoic acid receptors alpha, beta and gamma in F9 mouse teratocarcinoma cells. Differentiation *51*, 219-224.

Wueest, S., Mueller, R., Bluher, M., Item, F., Chin, A.S., Wiedemann, M.S., Takizawa, H., Kovtonyuk, L., Chervonsky, A.V., Schoenle, E.J.*, et al.* (2014). Fas (CD95) expression in myeloid cells promotes obesity-induced muscle insulin resistance. EMBO Mol Med *6*, 43-56.

Xiao, X., Gaffar, I., Guo, P., Wiersch, J., Fischbach, S., Peirish, L., Song, Z., El-Gohary, Y., Prasadan, K., Shiota, C., and Gittes, G.K. (2014). M2 macrophages promote beta-cell proliferation by up-regulation of SMAD7. Proc Natl Acad Sci U S A *111*, E1211-1220.

Yokota, A., Takeuchi, H., Maeda, N., Ohoka, Y., Kato, C., Song, S.Y., and Iwata, M. (2009). GM-CSF and IL-4 synergistically trigger dendritic cells to acquire retinoic acid-producing capacity. Int Immunol *21*, 361-377.

FIGURE LEGENDS

Figure 1

IL-33 Expression In Pancreatic Islets

(A and B) (A) Blood glucose and (B) plasma insulin levels during GTT in C57BL/6 and BALB/c mice. n = 25 mice each from 5 cohorts.

(C) Insulinogenic index defined as the ratio of the insulin to glucose areas under the curve during GTT. n = 25 mice each from 5 cohorts.

(D) Insulin release from islets isolated from C57BL/6 and BALB/c mice during GSIS. n = 13 each from 3 independent experiments.

(E) Gene expression of *Il33*, *Tslp* and *Il25* in islets isolated from C57BL/6 and BALB/c mice. n = 10 each from 3 independent experiments. n.d. = not detectable.

(F) Representative picture of *Il33* promoter-driven β-galactosidase expression in pancreata of $Il33^{+/+}$ wildtype (WT) and $Il33^{+/Gt}$ mice (n = 4). Black line indicates islet's perimeter.

(G) *Il33* gene expression in sort-purified islet $CD45^+$ immune cells and $CD45^-$ cell fraction isolated from pooled C57BL/6 females. n = 6 independent experiments.

(H) Representative plots of GFP and Epcam expression by islet cells isolated from $Il33^{gfp/wt}$ and C57BL/6 mice. n=3.

(I) Representative FSC/SSC profile of islet $CD45^+$, GFP^+ and GFP^- cell fractions (n=3).

(J) Histograms of Sca-1 expression by islet GFP^- and GFP^+ cells (n=2).

(K) Representative vimentin staining (n=2) in sort-purified islet Sca-1^- β cell-enriched cells (high FSC/SSC profile), other Sca-1^- cells and Sca-1^+ cells.

(L and M) IL-33 protein concentrations in (L) C57BL/6 and BALB/c mouse and (M) human islet cell lysates treated with IL-1β, glucose, bovine serum albumin (BSA) and/or BSA-Palmitate. n = 3 independent experiments and n = 5 donors, respectively.

Data are represented as the mean ± SEM. $*p < 0.05$, $**p < 0.01$, $***p < 0.001$; Statistical significance (*p*) was determined by one-way (L and M when normalized to baseline) or two-way

analysis of variance (ANOVA) (A, B, D and E) with Bonferroni's post-hoc test and Student's t test (C and G). See also Figure S1.

Figure 2

Islet IL-33-Responding Cells Are Resident Group 2 Innate Lymphoid Cells

(A) *Il1rl1* gene expression in sort-purified islet $CD45^+$ immune cells and $CD45^-$ cell fraction isolated from pooled C57BL/6 females. n = 6 independent experiments.

(B and C) Immune cell profiling of islets isolated from pools of C57BL/6 and BALB/c mice. Cell abundance is expressed as (B) percentage of total $CD45^+$ cells and (C) absolute cell number per 1000 islets. n = 3-5 independent experiments each (see complete gating strategy in Figure S2A).

(D) Mean fluorescence intensity (MFI) of T1/ST2 expressed on the surface of islet immune cells. n = 6-12 independent experiments.

(E) Representative plot of $GATA3^+$ILC2 and $ROR\gamma t^+$ILC3 among $CD45^+Lin^-CD90.2^+$ cells in BALB/c islets. n = 3 independent experiments.

(F) Histograms of T1/ST2 expression by ILC2 isolated from islets and exocrine stroma of the same mouse pancreas. n = 4 independent experiments.

(G) Representative picture (n = 4 mice) of C57BL/6 $Rag2^{-/-}$ mouse pancreas stained for CD45.2 (blue), KLRG1 (red), NKp46 (green) and DAPI (white). Blue dashed line indicates islet's perimeter.

(H) Cytokine concentrations in culture supernatants of 90 BALB/c islets (n = 19 each from 6 independent experiments) or 1000 sort-purified C57BL/6 pancreatic ILC2 (n = 12 each from 3 independent experiments) in response to IL-33 and IL-2.

(I) Representative plots and quantification of ILC2 in islets isolated from $Il33^{+/+}$ and $Il33^{Gt/Gt}$ mice. n = 4 cohorts.

Data are represented as the mean ± SEM. $*p < 0.05$, $**p < 0.01$, $***p < 0.001$; Statistical significance (p) was determined by one-way ANOVA (D) with Bonferroni's post-hoc test and Student's t test (A-C and I when normalized to baseline).

Figure 3

IL-33 Promotes Glucose Disposal And Insulin Secretion

C57BL/6 mice were treated with saline or IL-33 (500 ng) injection for one or three doses every other day.

(A-E) (A) Body weight (before and after treatment), inguinal white adipose tissue (IngWAT), epididymal (Epi)WAT and brown adipose tissue (BAT) mass, (B) fasting glycemia and blood glucose, (C) plasma insulin levels and (D) insulinogenic index during GTT in saline- and IL-33-treated mice. n = 20, 19 and 15 (except for BAT n = 6-7), respectively, from 5 cohorts. *p* represents comparison to saline group.

(E and F) Insulin release from islets isolated from saline- and IL-33-treated mice during (E) GSIS (n = 19 each from 4 independent experiments) and (F) potassium chloride (KCl)-induced insulin secretion assays (n = 12 each from 3 independent experiments).

(G) Quantification of insulin^{+} β cell area in pancreata of saline- and IL-33-treated mice. n = 9-10 mice from 3 cohorts (one section per animal).

(H) Blood glucose levels normalized to baseline during insulin tolerance test in saline- and IL-33-treated mice. n = 8 mice each from 2 cohorts.

(I and J) (I) Glucose infusion rate (GIR) and (J) tissue glucose uptake in skeletal (Sk.) muscle, IngWAT, EpiWAT and BAT during hyperinsulinemic-euglycemic clamps in saline- and IL-33-treated mice. n = 5-6 each from 2 cohorts.

(K) Blood glucose levels during GTT in saline- and IL-33-treated *Ucp1*$^{-/-}$ mice. n = 6-7 representative of 2 cohorts.

(L) Insulin release from islets isolated from *Il33*$^{+/+}$ and *Il33*$^{Gt/Gt}$ littermate mice during GSIS. n = 11 each from 3 cohorts.

Data are represented as the mean ± SEM. *p < 0.05, **p < 0.01, ***p < 0.001; Statistical significance (p) was determined by one-way (B, D and J) or two-way (B, C, E, F, L and K) ANOVA with Bonferroni's post-hoc test and Student's t test (K). See also Figure S3.

Figure 4

ILC2 Contribute To IL-33-Induced Insulin Secretion

(A) Absolute immune cell number per 1000 islets isolated from pooled saline- and IL-33-treated (three doses) C57BL/6 mice. n = 3 to 12 independent experiments.

(B) Gene expression of *Il13*, *Il5* and *Csf2* in islets isolated from saline- and IL-33-treated mice. n = 10-12 from 4 cohorts.

(C) Blood glucose levels in BALB/c WT, *Rag2*$^{-/-}$ and *Rag2*$^{-/-}$*γc*$^{-/-}$ mice treated with saline or three doses of IL-33 during GTT. n = 10-15 mice each from 3 cohorts.

(D) Insulin release during GSIS from islets isolated from saline- and IL-33-treated BALB/c WT (n = 12-13 each), *Rag2*$^{-/-}$ mice (n = 20 each) and *Rag2*$^{-/-}$*γc*$^{-/-}$ mice (n = 14-15 each) from 3-4 cohorts.

(E) Representative plots and quantification of ILC2 in islets isolated from Immunoglobulin G (IgG)- or anti-CD90.2-treated BALB/c *Rag2*$^{-/-}$ mice. n = 3 cohorts.

(F) Insulin release during GSIS from islets isolated from *Rag2*$^{-/-}$ treated with IgG or anti-CD90.2 antibody. n = 16 each from 3 cohorts.

(G and H) Sort-purified pancreatic ILC2 or PBS were transferred to IL-33-treated *Rag2*$^{-/-}$*γc*$^{-/-}$ mice. (G) Blood glucose levels during GTT (n = 3 mice) and (H) insulin release during GSIS (n = 16 from 4 mice) from 2 cohorts.

(I) Insulin release during GSIS of C57BL/6 islets treated with ILC2-conditioned media or control medium. n = 19 per group from 4 independent experiments.

Data are represented as the mean ± SEM. *p < 0.05, **p < 0.01, ***p < 0.001; Statistical significance (p) was determined by one-way (B) or two-way (C, D, F, H and I) ANOVA with

Bonferroni's post-hoc test and Student's t test (A and E when normalized to baseline). See also Figure S4.

Figure 5

IL-33 Regulates Retinoic Acid-Producing Capacities In Islet Myeloid Cells

(A) Gene expression of *Aldh1a2* in islets isolated from saline- and IL-33-treated mice (one and three doses of 500ng i.p.). n = 9-10 from 3 cohorts.

(B) Gene expression of *Aldh1a2* in sort-purified islet macrophages (MΦ) and dendritic cells (DC) isolated from saline- and IL-33-treated mice. n = 4 independent experiments.

(C and D) Histograms and frequencies of (C) $ALDH^+$ R1 MΦ and (D) $ALDH^+$ DC in islets isolated from saline- and IL-33 (three doses)-C57BL/6 WT treated mice. n = 5 cohorts. Islets treated with the ALDH inhibitory diethylaminobenzaldehyde (DEAB) were used as a negative control.

(E and F) Frequencies of (E) $ALDH^+$ R1 MΦ and (F) $ALDH^+$ DC in islets isolated from saline- and IL-33 (three doses)-treated BALB/c *Rag2*$^{-/-}$ and *Rag2*$^{-/-}$*γc*$^{-/-}$ mice. n = 3 cohorts.

(G and H) Gene expression of *Aldh1a2* in (G) sort-purified islet macrophages (n = 4 independent experiments) or (H) bone marrow-derived DC (BM-DC; n = 10 from 3 independent experiments) stimulated with recombinant IL-13 and Csf2.

(I) Gene expression of *Aldh1a2* in C57BL/6 islets treated with ILC2-conditioned media (CM) or control medium with or without anti(α)-IL-13 and α-Csf2 neutralizing antibodies. n = 8-9 per group from 3 independent experiments.

(J) Gene expression of *Aldh1a2* in islets isolated from BALB/c mice and stimulated with IL-2 and IL-33 *in vitro*. n = 9 per group from 3 independent experiments.

(K) Frequencies of $ALDH^+$ DC in islets isolated from *Il33*$^{+/+}$ and *Il33*$^{Gt/Gt}$ littermates. n = 3 cohorts.

Data are represented as the mean ± SEM. **p* < 0.05, ***p* < 0.01, ****p* < 0.001; Statistical significance (*p*) was determined by one-way ANOVA (A, C-H) and two-way ANOVA (I and K) with Bonferroni's post-hoc test and Student's t test (B and J). See also Figure S5.

Figure 6

IL-33-Induced Insulin Secretion Requires The Retinoic Acid-Precursor Vitamin A

(A) Insulin release during GSIS from islets treated with DMSO or all-*trans* RA *in vitro*. n = 15-16 each from 3 independent experiments.

(B) Gene expression of retinoic acid receptors in islets treated with DMSO or all-*trans* RA. n = 6 each from 2 independent experiments.

(C) Insulin release during GSIS from islets treated with ILC2-conditioned media (CM) or control medium in the presence of the retinoic acid receptor (RAR) β antagonist LE135 or DMSO. n = 12-13 each from 3 independent experiments.

(D-H) C57BL/6 mice fed a control chow (CD) or vitamin A deficient (VAD) diet were given saline or IL-33 (three doses).

(D) Frequencies and absolute number of ILC2 and eosinophils in islets isolated from IL-33-treated mice fed a CD or VAD. n = 3 from 3 cohorts.

(E) Gene expression of *Aldh1a2* in islets isolated from saline- and IL-33-treated mice fed a CD or VAD. n = 6-10 each from 4 cohorts.

(F) Insulinogenic index during GTT in saline- and IL-33-treated mice fed a CD or VAD. n = 11-13 mice each from 3 cohorts.

(G-H) Insulin release during (G) GSIS and (H) potassium chloride-stimulated insulin secretion assays from islets isolated from saline- and IL-33-treated mice fed a CD or VAD. n = 8-9 each from 2 cohorts.

Data are represented as the mean ± SEM. $*p < 0.05$, $**p < 0.01$, $***p < 0.001$; Statistical significance (*p*) was determined by one-way ANOVA (E and F) and two-way ANOVA (A-C, G and H) with Bonferroni's post-hoc test. See also Figure S6.

Figure 7

The IL-33/ILC2 Axis Is Altered During Chronic *Versus* Acute Islet Stress

(A) Gene expression of *Il33* in islets isolated from mice fed a normal chow diet (CD) or a high fat diet (HFD) for 3 and 7 months. n = 12-17 each from 3 cohorts.

(B) IL-33 protein concentrations in islet cell lysate of CD- or HFD-fed mice for 3 months. n = 6-8 each from 2 cohorts.

(C) Representative plots, frequencies and absolute number of ILC2 in islets isolated from mice fed a CD or a HFD for 3 months. Gated on $CD45^+Lin^-CD90.2^+$ cells. n = 4 cohorts.

(D) Gene expression of *Aldh1a2* in islets isolated from mice fed a CD or a HFD for 3 and 7 months. n = 12-17 each from 3 cohorts.

(E and F) (E) Blood glucose and (F) plasma insulin levels during GTT in mice fed a HFD for 7 months and treated with saline or IL-33 (three doses). Ratio of insulin secretion between times 0 and 15 min is shown. n = 10 mice each from 2 cohorts.

(G) Gene expression of *Il33* in islets isolated from buffer or streptozotocin (STZ)-treated mice on day 15 post-injection. n = 6-7 each from 2 cohorts.

(H) Representative plot, frequencies and absolute number of ILC2 in islets isolated from buffer or STZ-treated mice on day 15 post-injection. Gated on $CD45^+Lin^-CD90.2^+$ cells. n = 3 cohorts.

(I) Gene expression of *Aldh1a2* in islets isolated from buffer or STZ-treated CD mice on day 15 post-injection. n = 6-7 each from 2 cohorts.

(J) C57BL/6 mice were treated with STZ on day 0. From day 6, mice were administered saline or IL-33 (three doses) every other day. Fasting blood glucose levels and body weight were monitored. n = 12-13 mice from 3 cohorts.

(K) C57BL/6 $Rag2^{-/-}$ mice were given STZ on day 0 and treated with IgG or anti(α)-CD90.2 antibody on days 6 and 8. Fasting blood glucose levels were monitored and normalized to baseline. n = 9-10 mice from 3 cohorts.

Data are represented as the mean ± SEM. *$p < 0.05$, ***$p < 0.001$; Statistical significance (p) was determined by two-way ANOVA (A, D-F) with Bonferroni's post-hoc test and Student's t test (B, C, F- J). See also Figure S7.

STAR★METHODS

KEY RESOURCES TABLE

CONTACT FOR REAGENT AND RESOURCE SHARING

Further information and requests for resources and reagents should be directed to and will be fulfilled by the Lead Contact, Elise Dalmas (elise.dalmas@unibas.ch).

EXPERIMENTAL MODEL AND SUBJECT DETAILS

Mice

Male (and where indicated, female) C57BL/6 and BALB/c wildtype mice were either purchased from Charles River and Janvier Labs, respectively, or were bred in-house. C57BL/6 *Rag2*$^{-/-}$ mice were from Taconic and bred in-house. BALB/c *Rag2*$^{-/-}$ mice were a gift from A. Rolink (University of Basel, Switzerland). BALB/c *Rag2*$^{-/-}$*γc*$^{-/-}$ (C;129S4-*Rag2*$^{tm1.1Flv}$ Il2rg$^{tm1.1Flv}$/J) were purchased from Jackson Laboratories. *IL33*$^{Gt/Gt}$ mice (*Il33*$^{Gt(IST10946B6-Tigm)}$) were generated with insertion of a gene trap cassette containing the LacZ (bgeo) reporter into intron 1 of the *Il33* locus as described previously (Pichery et al., 2012). *Il33*$^{Gt/Gt}$ mice were first backcrossed for 4 generations with C57BL/6J mice to obtain >98% purity using speed congenics. *Il33*$^{Gt/Gt}$, *Il33*$^{Gt/+}$ and *Il33*$^{+/+}$ mice were all littermates. IL33 reporter mice (*Il33*$^{gfp/wt}$) were derived from the *Il33*$^{-/-}$ mice (*Il33*^{tm1Snak}; (Oboki et al., 2010) obtained by the RIKEN Center for Developmental Biology (Accessory Number: CDB0631K; http://www.cdb.riken.jp/arg/mutant%20mice%20list.html) and generated by intercrossing *Il33*$^{-/-}$ mice with the ZP3-Cre germ line deleter strain to remove the neomycin cassette as previously described (Kallert et al., 2017). *Ucp1*$^{-/-}$ mice (B6.129-Ucp1^{tm1Kz}/J) were purchased from the Jackson Laboratory. Unless otherwise indicated, all mice were fed a chow diet (3436, Provimi Kliba) and sacrificed at 10-16 weeks of age. For diet-induced obesity experiments, 4-week-old C57BL/6 mice were fed a high fat diet (D12331, Research Diets; containing 58, 26 and 16% calories from fat, carbohydrate and protein, respectively) for 3 to 7 months. Mice that did not gain weight under high fat diet were excluded before experimentation. For vitamin A deprivation experiments, 6-week-old C57BL/6 mice were fed a vitamin A deficient diet or the corresponding vitamin A sufficient control diet for 10 weeks (E15311 and E15000; Ssniff special diets GmbH). All animal experiments were conducted according to the Swiss Veterinary Law and Institutional Guidelines and were approved by the Swiss Authorities. All animals were housed under specific pathogen-free conditions, in a 22°C temperature-controlled room with a 12h light – 12h dark cycle

and had free access to food and water. All metabolic experiments (glucose and insulin tolerance tests, GSIS and clamps) were performed with littermate mice.

Human pancreatic islets

Human islets were isolated from pancreata of cadaver organ donors at the islet transplantation center of Lille (France) in accordance with the local Institutional Ethical Committee and were provided by the research distribution program through the European Consortium for Islet Transplantation, under the supervision of the Juvenile Diabetes Research Foundation (31-2012-783). Islets were cultured in CMRL-1066 medium (GIBCO) containing 5 mmol/l streptomycin, 2 mM glutamax and 10% FCS (Invitrogen) in humid environment containing 5% CO2. In this study, islets were isolated from five different donors (2 women / 3 men) of 54.4 ± 2.4 years old with a body mass index of 29.2 ± 3.8 kg/m^2.

METHOD DETAILS

Mouse pancreatic islets

To isolate mouse islets, pancreata were perfused through the common bile duct with a HBSS collagenase solution (1.4 g/L; collagenase type 4 Worthington) and digested in the same solution in a 37°C water bath for 26-28 min. After shaking for 15 seconds, pancreata were washed three times with HBSS supplemented with 0.5% bovine serum albumin (BSA) and filtrated through 500 µm and 70 µm cell strainers (Corning). Islets were retained on the 70 µm cell strainer while the cell mixture passing through the 70 µm cell strainer represented the exocrine stoma. Islets were double handpicked into a Petri dish with RPMI-1640 (GIBCO) containing 11.1 mM glucose, 100 units/ml penicillin, 100 µg/ml streptomycin, 2 mM Glutamax, 50 µg/ml gentamycin, 10 µg/ml Fungison and 10 % FCS (Invitrogen). Islets were used directly for FACS analysis, RNA isolation or cell culture in humid environment containing 5 % CO_2.

***In vitro* islet treatment**

For *Il33* gene expression analyses, 80 handpicked mouse or 2 µL of human islet preparation were cultured on extracellular matrix-coated 24-well plates and treated overnight with recombinant mouse or human IL-1β (10 ng/mL; R&D systems), 33.3 mM of glucose, low endotoxin BSA (Sigma-Aldrich) and/or BSA-coated sodium palmitate (0.5mM; Sigma-Aldrich) before lysis for RNA isolation. For IL-33 protein measurement, 200 handpicked mouse islets or 4 µL of human islet preparation were cultured in suspension in a 96-well plate with similar treatments. After 24h

culture, islet-free supernatants were stored at -80°C until analysis. For extraction of the whole-protein fraction of islets, samples were homogenized in lysis buffer (20mM Tris pH 7.5; 150mM NaCl; 10% glycerol; 1% Triton X-100; 1% Na_3VO_4; 1% NaF; 0.5% PMSF and 1 mM EDTA) supplemented with a protease inhibitor cocktail (Roche). When indicated, mouse cultured islets were treated with 1 µM of all-*trans* retinoic acid (R2625; Sigma-Aldrich) for 24h, 2 µM of the synthetic RARβ receptor antagonist LE135 (SML0809; Sigma-Aldrich) for 24h or the neutralizing anti-mouse IL-13 (0.05 µg/mL) and anti-mouse GM-CSF (1.25 µg/mL) Functional Grade Purified antibodies and corresponding isotypes for 48h (Thermo Fisher Scientific). BALB/c islets were stimulated *ex vivo* with IL-2 and IL-33 (10 ng/mg; Thermo Fisher Scientific) for 72h.

***In vitro* glucose- and potassium chloride-stimulated insulin secretion assays**

For *ex vivo* insulin secretion stimulation assays, mouse islets were cultured for 24h and then pre-incubated for 30 min in modified Krebs-Ringer bicarbonate buffer (KRB; 115 mM NaCl, 4.7 mM KCl, 2.6 mM $CaCl_2$ $2H_2O$, 1.2 mM KH_2PO_4, 1.2 mM $MgSO_4$ $2H_2O$, 10 mM HEPES, 0.5 % bovine serum albumin, pH 7.4) containing 2.8 mM glucose. KRB was then replaced by KRB with 2.8 mM glucose and collected after 1h to determine the basal insulin release. This was followed by 1h incubation in KRB with 16.7 mM glucose (GSIS) or with KRB with 2.8 mM glucose supplemented with 25 mM of potassium chloride to determine the glucose- or potassium chloride-stimulated insulin release. After supernatant collection, islet protein content was extracted with 0.18 N hydrochloride acid in 70% ethanol to measure insulin content (20 islets in 500 µL). For GSIS following an *in vitro* treatment, islets were resting for 48h and then treated for 24h with all-*trans* retinoic acid or 48h with ILC2-conditioned or control media before GSIS.

***In vivo* Glucose and Insulin Tolerance Tests**

For glucose tolerance tests (GTT), mice were fasted for 6h in the morning and then injected with glucose (2 g per kg of body weight) intraperitoneally (i.p.). For insulin tolerance tests, mice were fasted for 3h in the morning and i.p. injected with human insulin (Novorapid, Novo Nordisk) (1U per kg of body weight) diluted in saline solution. Blood glucose was sampled from the mouse tail vein every 15–30 min following glucose or insulin injection and measured using a glucometer (Freestyle, Abbott Diabetes Care Inc.).

Glucose clamp studies

Glucose clamp studies were performed in freely moving mice as previously described (Wueest et al., 2014). Steady state glucose infusion rate was calculated once glucose infusion reached a constant rate with blood glucose levels at 5 mmol/l (80-90 min after the start of insulin infusion). Thereafter, blood glucose concentration was kept constant at 5 mmol/l for 15-20 min and glucose infusion rate was calculated. Glucose infusion rate and hepatic glucose production were calculated as previously described (Wueest et al., 2014). In order to assess tissue specific glucose uptake, a bolus (10 µCi) of 2-[1-14C] deoxyglucose was administered via catheter at the end of the steady state period. Blood was sampled 2, 15, 25 and 35 min after bolus delivery. Area under the curve of disappearing plasma 2-[1-14C] deoxyglucose was used together with tissue-concentration of phosphorylated 2-[1-14C] deoxyglucose to calculate glucose uptake.

In vivo IL-33 and anti-CD90.2 antibody treatments

Carrier-free recombinant murine IL-33 (Biolegend) was administered in 100 µL sterile saline by i.p. injection for one or three doses every other day at 500 ng per dose in chow diet mice. Mice fed a high fat diet received either saline or IL-33 for three doses every other day at 20 µg per kg of body weight. Metabolic tests were performed the day after the last injection. Mice were sacrificed one or two days after the last injection. For streptozotocin-induced diabetic C57BL/6 mice, only hyperglycemic mice (*i.e.* fasting blood glucose > 11 mM) were injected with IL-33 (starting from day 6 after streptozotocin injection). Anti-CD90.2 (30-H12; 250 µg) antibody or corresponding IgG2b (RTK4530) (Biolegend) was administered in 125 µL sterile Phosphate Buffer Solution by i.p. injection twice every other day into BALB/c *Rag2*$^{-/-}$ mice or streptozotocin-induced diabetic C57BL/6 *Rag2*$^{-/-}$ mice (starting from day 6 after streptozotocin injection).

Flow cytometry

Handpicked islets were isolated and pooled together from at least 3 mice per condition. To obtain single cells, islets were gently dispersed with a 0.0125% trypsin-EDTA (GIBCO) solution for 2 min in a 37°C water bath, washed with cold FACS buffer (PBS with 0.5% BSA and 5 mM EDTA), centrifuged at 300 x g, 4°C for 5 min and resuspended in FACS buffer. After 15 min incubation with an Fc blocker (93; Thermo Fisher Scientific), single islet cells were stained with the appropriate antibodies or isotypes for 30 min at 4°C in the dark. The following antibodies were used: anti-CD45 (30-F11), anti-F4/80 (BM8), anti-CD11c (N418), anti-I-A/I-E (MHC-II) (M5/114.15.2), anti-CD3 (145-2C11), anti-B220 (RA3-6B2), anti-NKp46 (29A1.4), anti-Ly6G (1A8 – Ly6g), anti-CD90.2 (53-2.1), anti-KLRG1 (2F1), anti-CD103 (2E7) and anti-Sca-1 (D7) (from

Thermo Fisher Scientific or Biolegend); anti-SIGLEC-F (E50-2440) (from BD bioscience) and anti-T1/ST2 (DJ8) (from mdbioproducts). ILC2 and ILC3 were identified based on the absence of PE-labeled lineage markers: anti-F4/80 (BM8), anti-CD11b (M1/70), anti-CD11c (N418), anti-Ly6G (RB6-8C5), anti-CD3 (145-2C11), anti-CD4 (GK1.5), anti-CD8a (53-6.7), anti-TCR beta (H57-597), anti-gamma delta TCR (eBioGL3), anti-CD19 (eBio1D3), anti-CD45R (RA3-6B2), anti-NKp46 (29A1.4), anti-NK1.1 (PK136) for C57BL/6 mice, anti-CD49b (DX5) for BALB/c mice and anti-Ter119 (Ter119) (all from Thermo Fisher Scientific). Anti-NKp46 was excluded from the lineage cocktail for the comparative study of ILC2/ILC3. $DAPI^+$ cells and doublet were excluded from all analyses. For the detection of transcription factors, cells were fixed and stained using the Foxp3-staining kit (Thermo Fisher Scientific) according to the manufacturer's instructions and using anti-GATA3 (TWAJ) and anti-RORγ(t) (B2D) antibodies and a fixable viability dye (all from Thermo Fisher Scientific). For quantification of β and α cells in islets, cells were fixed and stained with anti-insulin (C27C9; Cell Signaling) and biotinylated anti-glucagon antibodies (Abcam). Multiparameter analyses were performed on a LSR-Fortessa flow cytometer (BD Bioscience) and analyzed with FlowJo software (Tree Star). For islet cell fraction sorting, anti-CD45 (30-F11) and anti-Sca-1 (D7) antibodies were used (from Thermo Fisher Scientific) and sorted with a FACS ARIA III cell sorter (BD Biosciences) using FACS Diva software (BD Biosciences).

Aldehyde dehydrogenase activity

Aldehyde dehydrogenase (ALDH) activity was determined using the ALDEFLUOR staining kit (StemCell Technologies) according to the manufacturer's instructions. Briefly, dispersed islet cells were divided into two tubes: one test and one control. In the control tube, ALDH inhibitor diethylaminobenzaldehyde (DEAB) was added and incubated for 15 min at 37°C. Then, fluorescent ALDH reagent was added in both tubes for 35 min at 37°C. Cells were washed twice and incubated with appropriate antibodies for FACS analysis.

Sort-purification of pancreatic ILC2

Whole pancreata of C57BL/6 mice were collected and pancreatic lymph nodes were removed under a stereomicroscope. Pancreata were cut into small pieces with razor blades and washed in fresh ice cold PBS. Pancreas pieces were incubated in 1.5 mL DMEM (GIBCO) containing 1 mg/ml Collagenase D (Roche) and 0.025 mg/mL DNAse I (Roche) at 37ºC for 15 min. After incubation, pancreas pieces were washed with DMEM and supernatant was collected and passed through a 70 µm cell strainer (Corning). These steps were repeated 3 to 4 times. Isolated cells were washed with PBS and purified using a Percoll (GE Healthcare) gradient (40%/80%) at 20°C and 630 x g

for 30 min. Cells of the interphase were collected and washed with PBS containing 3% FCS (Gibco Life Technologies). Pancreatic ILC2 identified as Lin-CD90.2^{+}Sca-1^{+}CD25^{+} cells were sorted with a FACS Aria (BD Biosciences) and re-analysis showed that cell purity was > 95%.

In vitro stimulation of pancreatic ILC2

For ILC2-conditioned media, approximately 2000 ILC2 were stimulated for 72h in RPMI containing 10% FBS with recombinant mouse IL-33 (10 ng/mL; Biolegend) and IL-2 (10 ng/mL; Thermo Fisher Scientific) in 96-well round bottom plates (Falcon) at 37°C and 10% CO_2. Supernatant was recovered and stored at -80°C for further experiments. For control medium, cell-free RPMI containing 10% FBS supplemented with the cytokines was incubated for 72h in the same conditions.

ILC2 transfer

Pancreatic ILC2 were purified from C57BL/6 mice that received *i.p.* three doses of IL-33 (500ng) every other day. 3 x 10^5 cells or PBS were immediately transferred to recipient *Rag2*$^{-/-}$*γc*$^{-/-}$ mice by a single intravenous injection. 2h later and the next 2 days, recipient mice were treated with three doses of IL-33 (500ng) before performing GTT and islet isolation for *ex vivo* GSIS assays.

Histological analyses

For β-Galactosidase detection, pancreata from *Il33*$^{Gt/+}$ and *Il33*$^{+/+}$ littermates were embedded in OCT Tissue Tek and frozen in liquid nitrogen. Pancreas sections were fixed and stained with chromogenic substrate X-Gal overnight using a LacZ Tissue staining kit (InvivoGen) according to the manufacturer's instructions. Sections were counterstained by nuclear Fast Red (Sigma), mounted with Mounting medium (Dako) and analyzed with a widefield microscope (Olympus BX63 Apollo). For β cell area analysis, pancreata of saline- and IL-33-treated mice were fixed overnight in 4% paraformaldehyde at 4°C, followed by paraffin embedding. Sections were deparaffinized, re-hydrated and incubated overnight at 4°C with Guinea pig anti-insulin (Dako; A0564), followed by detection with Alexa657-conjugated Goat anti–guinea pig IgG (Thermo Fischer Scientific), counterstained with DAPI and mounted with Mounting medium (Dako). Pancreas sections were analyzed using a Hamamatsu flash 4.0 camera with a 4x Nikon Objective NA 0.2 and automatically scanned using a Nikon NiE with Prior PL-200 slide loading robot. Insulin^{+} area and distribution were calculated with NIS-Elements software (Nikon). For immunofluorescence staining of ILC2, pancreata of C57BL/6 *Rag2*$^{-/-}$ mice were embedded in OCT Tissue Tek and frozen in liquid nitrogen. Sections were fixed for 5 min in acetone at room temperature. They were then blocked

with PBS containing 1% BSA (Sigma-Aldrich) for 30 min at room temperature and stained with Alexa657-conjugated anti-CD45.2 (104) and PE-conjugated anti-KLRG1 (2F1-KLRG1) from Biolegend and anti-NKp46 (R&D systems, AF2225) overnight at 4°C, followed by detection with Alexa488-conjugated Donkey anti-goat IgG (Thermo Fisher scientific) for 1h at room temperature and counterstained with DAPI. The slices were mounted (Fluoromount-G, Thermo Fisher Scientific) and analyzed with a widefield microscope (Leica DMI 4000).

Immunocytochemistry of islet cells

For staining of mouse islet cells, islet Sca-1$^+$ cells and Sca-1$^-$ cells were sort-purified; Sca-1$^-$ cells were further separated between cells with a high FSC/SSC profile that are enriched in β cells and the rest. Following cytospin (Hettich) onto glass Polysine^{TM} slides, cells were fixed with 4% paraformaldehyde (Sigma Aldrich) for 10 min, permeabilized with 0.1% Triton-X-100 for 5 min, blocked with PBS supplemented with 0.1% Tween 20, 1% BSA (Sigma Aldrich) and 0.3 M glycine for 30 min at room temperature. Cells were stained with Rabbit anti-Vimentin (Abcam; EPR3776) overnight at 4°C, followed by detection with Alexa488-conjugated Donkey anti-rabbit IgG (Biolegend) and counterstaining with DAPI, mounted with Mounting medium (Dako) and analyzed with a widefield microscope (Olympus BX63 Apollo).

Bone marrow-derived dendritic cells

4 x 10^6 bone marrow cells per well were cultured in a 6 well plate (Nunc) in supplemented IMDM (Sigma Aldrich) in the presence of 200 ng/ml FMS-like tyrosine kinase ligand (FLT3l, A. Rolink, University of Basel, Switzerland) at 37ºC and 10% CO_2 as previously described (Brasel et al., 2000). After 6-7 days, BM-DCs were harvested, washed with PBS and used for overnight stimulation with IL-13 and Csf2 (10 ng/mL; Thermo Fisher Scientific) or IL-33 (10 ng/mL ; Biolegend). Cells were harvested afterwards and used for RNA isolation.

Streptozotocin-induced β cell death

Streptozotocin (Sigma-Aldrich) was dissolved in citrate buffer (pH 4.5) and was injected once i.p. into 6 hour-fasted C57BL/6 mice (150 mg per kg of body weight) or C57BL/6 *Rag2*$^{-/-}$ mice (120 mg per kg of body weight).

In situ pancreatic perfusion

In situ pancreatic perfusion was performed in anesthetized mice treated with saline or IL-33 (three doses) as previously described(Maechler et al., 2002) with a perfusion rate of 1.5 ml/min (Maechler et al., 2002).

Protein measurement assays

Insulin concentrations were determined using a mouse/rat insulin kit (Mesoscale Discovery) according to the manufacturer's instructions. Mouse Csf2, IL-5 and human IL-33 concentrations were measured using the mouse GM-CSF Tissue Culture Kit, the V-plex mouse IL-5 and the U-plex human IL-33 (Mesoscale Discovery) according to the manufacturer's instructions. Mouse IL-33 was measured using the U-plex mouse IL-33 (Mesoscale Discovery); protocol was improved to achieve a lower limit of detection (LLOD) of 0.31 ± 0.07 pg/mL (Mean ± SD; n = 4). Mouse IL-13 was measured using mouse IL-13 Platinum ELISA (Thermo Fisher Scientific) according to the manufacturer's instructions.

RNA extraction and qRT-PCR

Total RNA was extracted using the Nucleo Spin RNA II Kit (Machery Nagel) or RNeasy Mini Kit (QIAGEN) for islets and bone marrow-derived dendritic cells, RNeasy Lipid Tissue (QIAGEN) for epididymal adipose tissue and PureLink RNA Micro Scale Kit (Invitogren) for FACS-sorted cells. cDNA was prepared with random hexamers (Microsynth) and Superscript II (Invitrogen) according to manufacturer's instructions. Gene expression was determined with TaqMan assays and the real time PCR system 7500 (Applied Biosystems). Data were normalized with the geometrical mean of 18S and β actin mRNA (18S was used for human samples) and quantified using the comparative 2-ΔΔCT method. The following TaqMan assays (ThermoFisher scientific) were used: *18s*: Mm99999901; *Actb*: Mm00607939; *Acta2*: Mm00725412; *Aldh1a2*: Mm00501306; *Areg*: Mm00437583; *Ccl2*: Mm00441242; *Csf2*: Mm01290062; *Cxcl1*: Mm00433859; *Emr1*: Mm00802529; *Flt3*: Mm00439016; *Gcg*: Mm00801714; *Ifng*: Mm01168133; *Il10*: Mm01288386; *Il13*: Mm00434204; *Il1b*: Mm00434228; *Il1rl1*: Mm00516117; *Il4*: Mm00445258; *Il5*: Mm00439646; *Il22*: Mm01226722; *Il25*: Mm00499822; *IL33*: Hs01125943; *Il33*: Mm00505403; *Ins2*: Mm00731595; *Rara*: Mm01296312; *Rarb*: Mm01319677; *Rarg*: Mm00441091; *Rxra*: Mm00441185; *Tgfb*: Mm01178820; *Tslp*: Mm01157588; *Vim*: Mm01333430.

QUANTIFICATION AND STATISTICAL ANALYSIS

Data were routinely presented as mean ± standard error of mean (SEM). Significance was assessed by the methods specified in each individual figure legend using GraphPad Prism 7 (GraphPad Software). "n" numbers indicate biological replicates for *in vitro* experiments or number of mice for *in vivo* studies. Outliers were identified according to the two standard deviation method.

Figure 1

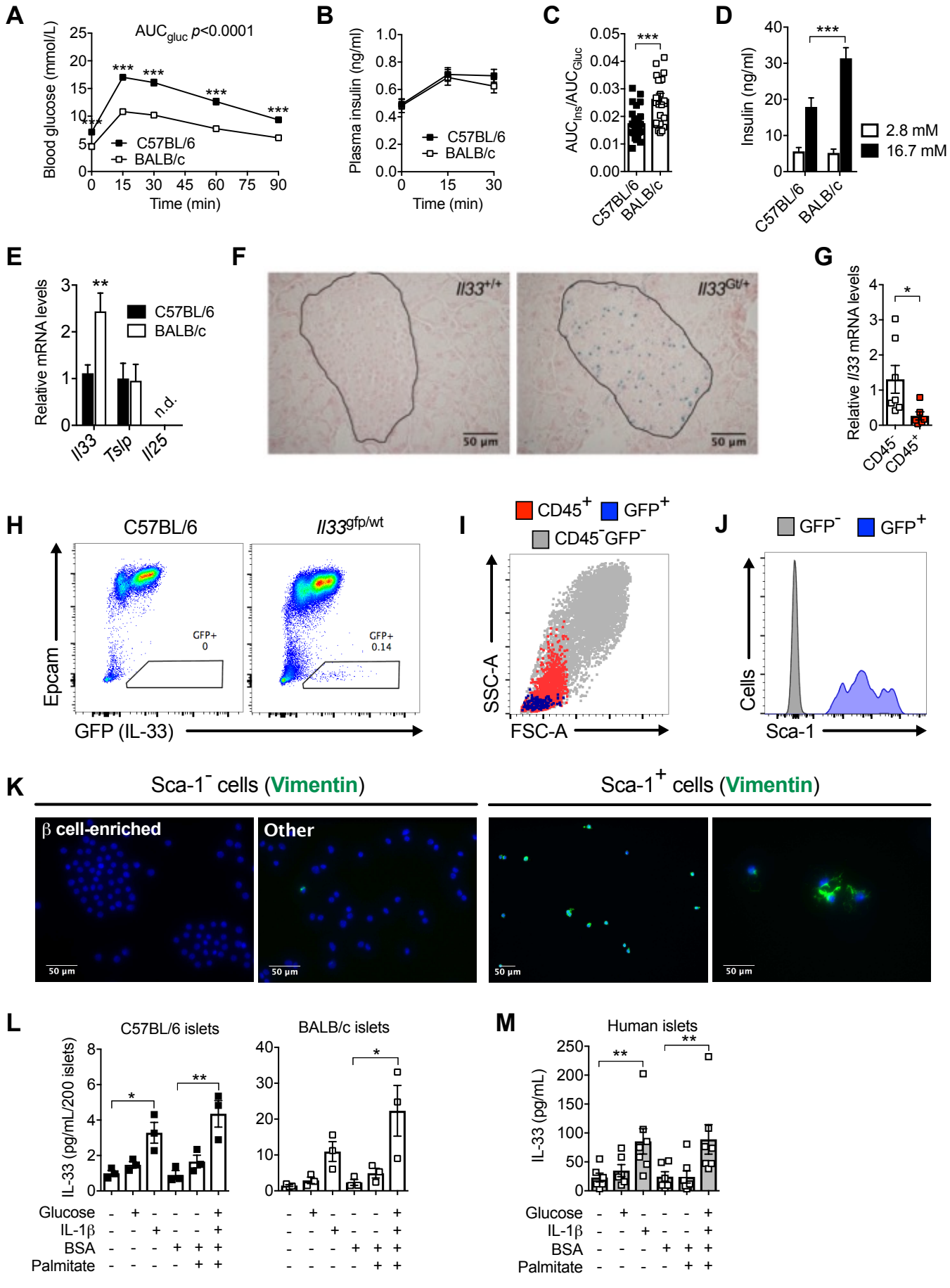
A
AUC$_{gluc}$ p<0.0001
Blood glucose (mmol/L)
Time (min)
C57BL/6
BALB/c
B
Plasma insulin (ng/ml)
Time (min)
C57BL/6
BALB/c
C
AUC$_{Ins}$/AUC$_{Gluc}$
C57BL/6
BALB/c
D
Insulin (ng/ml)
2.8 mM
16.7 mM
C57BL/6
BALB/c
E
Relative mRNA levels
C57BL/6
BALB/c
Il33
Tslp
Il25
n.d.
F
Il33+/+
Il33Gt/+
50 µm
G
Relative Il33 mRNA levels
CD45-
CD45+
H
C57BL/6
Il33gfp/wt
Epcam
GFP (IL-33)
GFP+ 0
GFP+ 0.14
I
CD45+ GFP+
CD45-GFP-
SSC-A
FSC-A
J
GFP- GFP+
Cells
Sca-1
K
Sca-1- cells (Vimentin)
Sca-1+ cells (Vimentin)
β cell-enriched
Other
50 µm
L
C57BL/6 islets
BALB/c islets
IL-33 (pg/mL/200 islets)
Glucose
IL-1β
BSA
Palmitate
M
Human islets
IL-33 (pg/mL)
Glucose
IL-1β
BSA
Palmitate

Figure 2

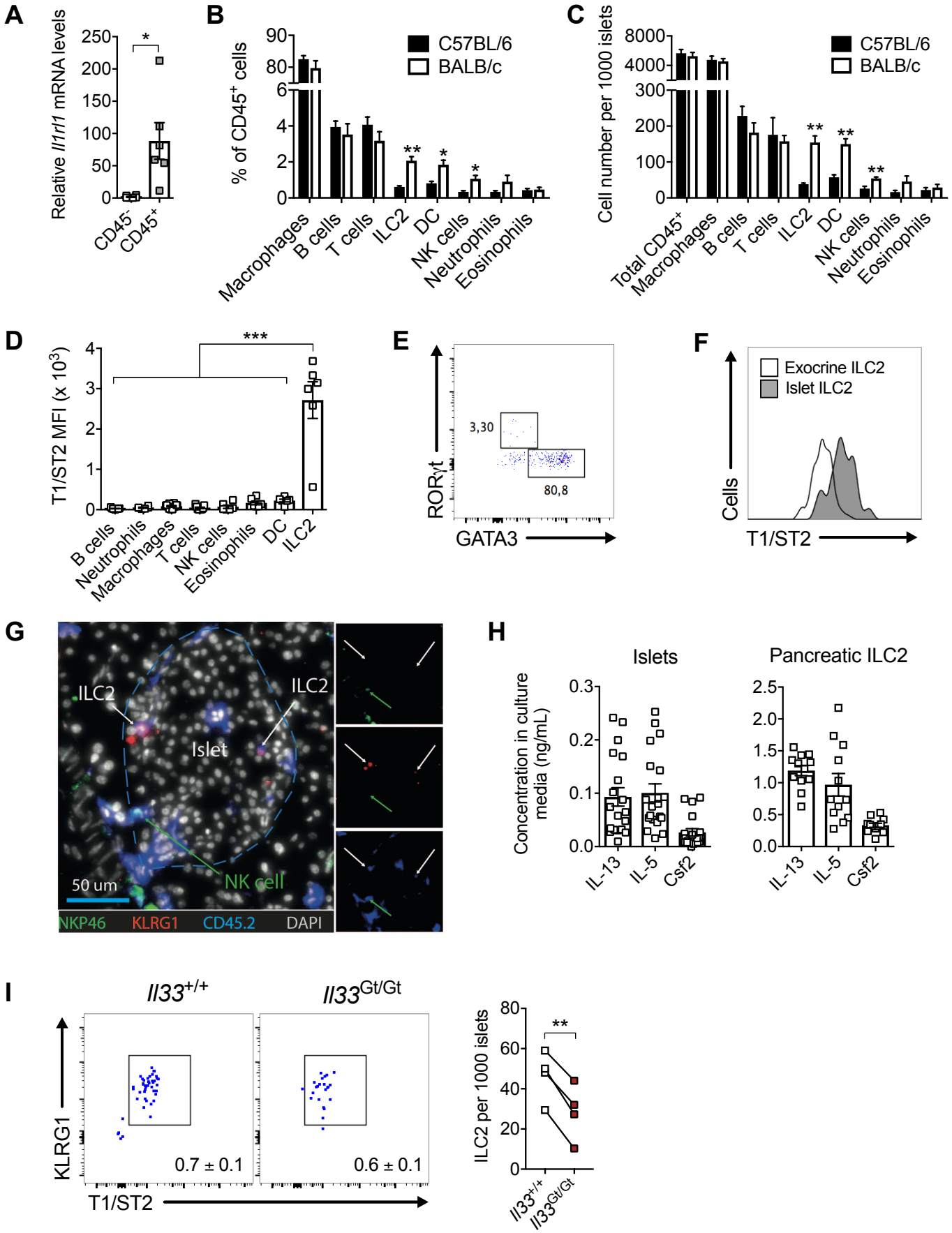
A
Relative Il1rl1 mRNA levels
CD45-
CD45+
B
% of CD45+ cells
C57BL/6
BALB/c
Macrophages
B cells
T cells
ILC2
DC
NK cells
Neutrophils
Eosinophils
C
Cell number per 1000 islets
Total CD45+
D
T1/ST2 MFI (x 10^3)
E
RORγt
GATA3
3,30
80,8
F
Exocrine ILC2
Islet ILC2
Cells
T1/ST2
G
ILC2
Islet
NK cell
50 um
NKP46
KLRG1
CD45.2
DAPI
H
Islets
Pancreatic ILC2
Concentration in culture media (ng/mL)
IL-13
IL-5
Csf2
I
Il33+/+
Il33Gt/Gt
KLRG1
T1/ST2
0.7 ± 0.1
0.6 ± 0.1
ILC2 per 1000 islets

Figure 3

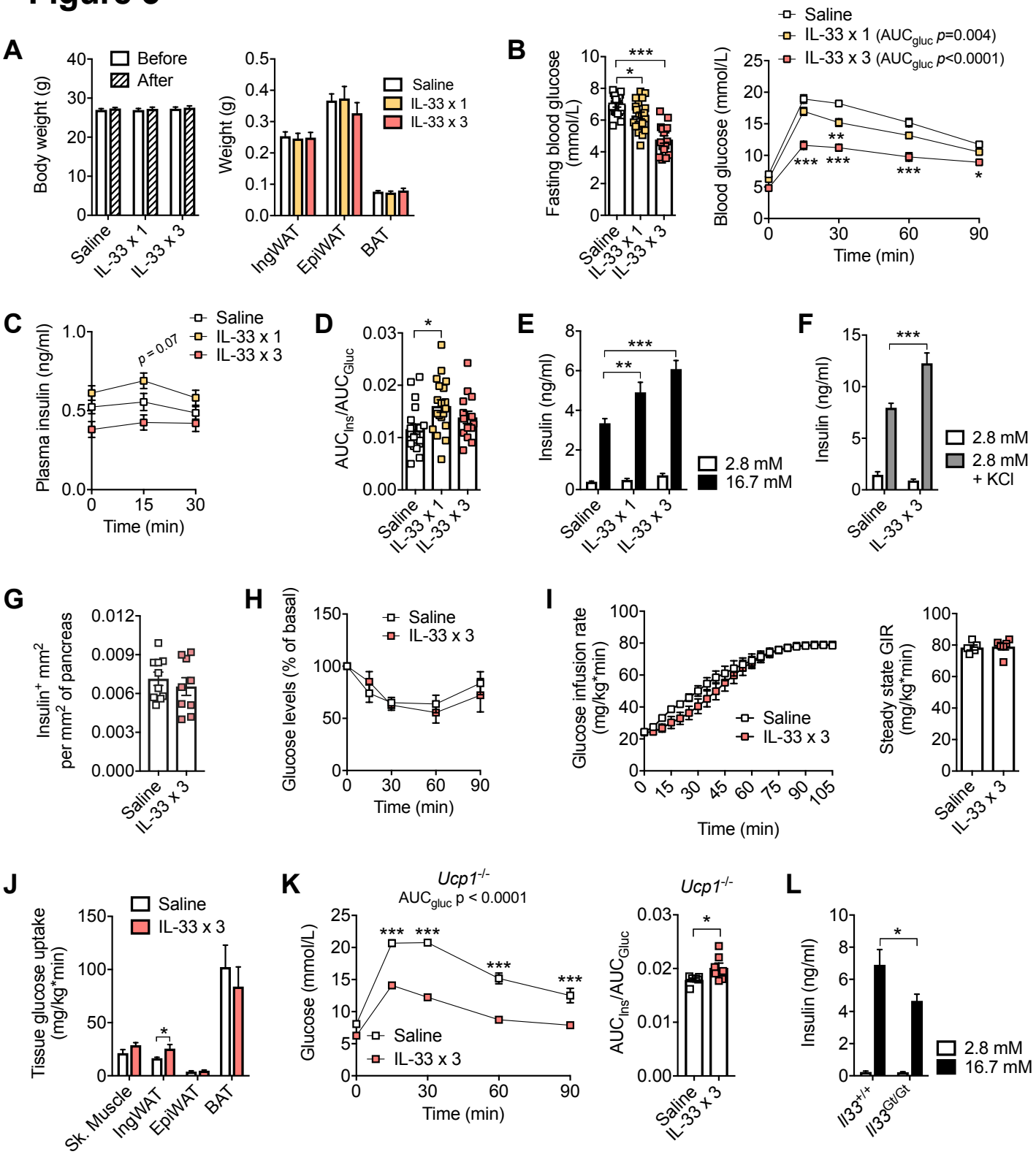
A
Body weight (g)
Before
After
Saline
IL-33 x 1
IL-33 x 3
Weight (g)
IngWAT
EpiWAT
BAT
B
Fasting blood glucose (mmol/L)
Blood glucose (mmol/L)
Saline
IL-33 x 1 (AUCgluc p=0.004)
IL-33 x 3 (AUCgluc p<0.0001)
Time (min)
C
Plasma insulin (ng/ml)
p = 0.07
Time (min)
D
AUCIns/AUCGluc
E
Insulin (ng/ml)
2.8 mM
16.7 mM
F
Insulin (ng/ml)
2.8 mM
2.8 mM + KCl
G
Insulin+ mm2 per mm2 of pancreas
H
Glucose levels (% of basal)
Time (min)
I
Glucose infusion rate (mg/kg*min)
Time (min)
Steady state GIR (mg/kg*min)
J
Tissue glucose uptake (mg/kg*min)
Sk. Muscle
IngWAT
EpiWAT
BAT
K
Ucp1-/-
AUCgluc p < 0.0001
Glucose (mmol/L)
Time (min)
Ucp1-/-
AUCIns/AUCGluc
L
Insulin (ng/ml)
2.8 mM
16.7 mM
Il33+/+
Il33Gt/Gt

Figure 4

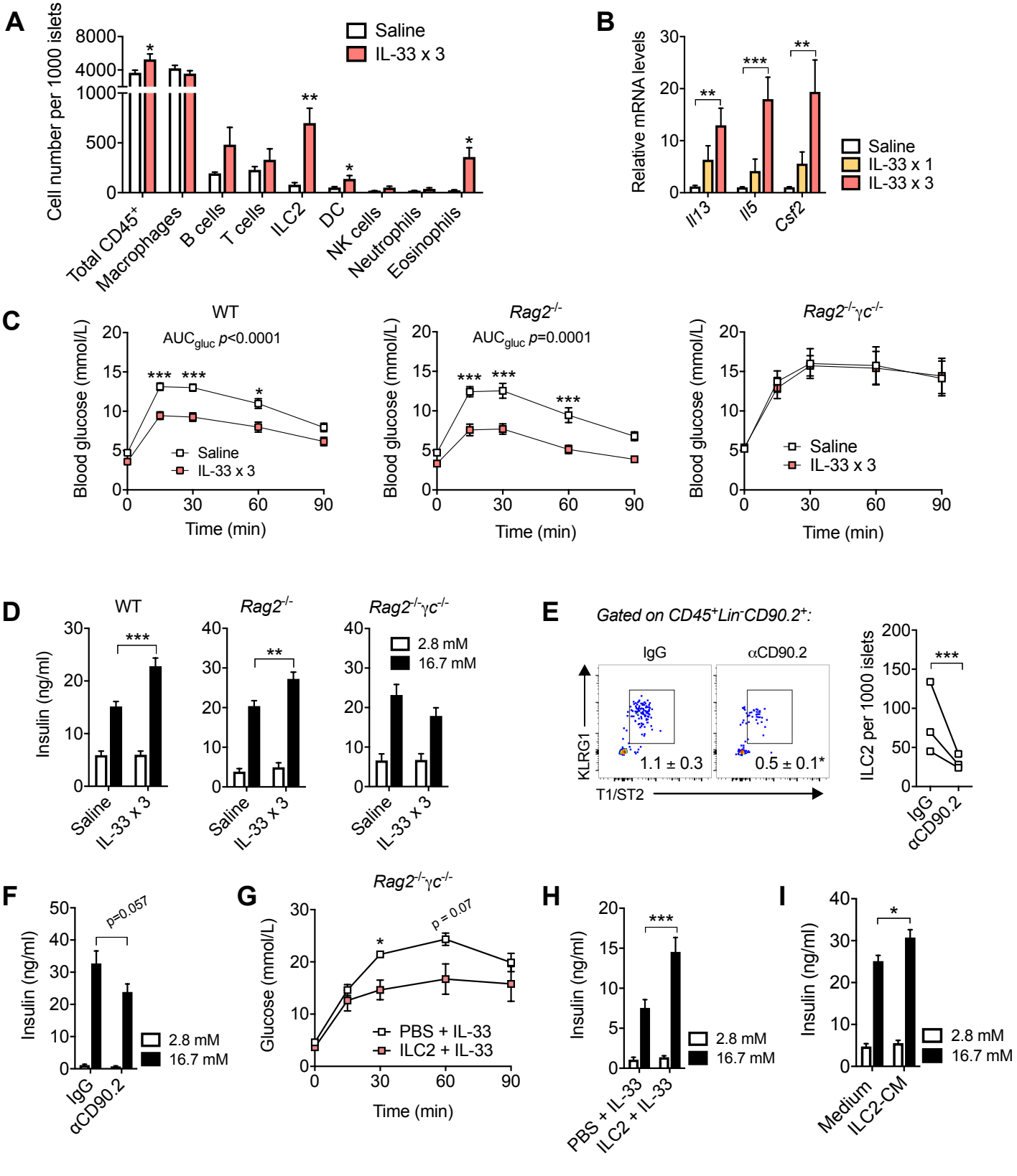
A
Cell number per 1000 islets
Saline
IL-33 x 3
Total CD45+
Macrophages
B cells
T cells
ILC2
DC
NK cells
Neutrophils
Eosinophils
B
Relative mRNA levels
Saline
IL-33 x 1
IL-33 x 3
Il13
Il5
Csf2
C
WT
Rag2-/-
Rag2-/-γc-/-
AUCgluc p<0.0001
AUCgluc p=0.0001
Blood glucose (mmol/L)
Time (min)
Saline
IL-33 x 3
D
WT
Rag2-/-
Rag2-/-γc-/-
Insulin (ng/ml)
2.8 mM
16.7 mM
E
Gated on CD45+Lin-CD90.2+:
IgG
αCD90.2
KLRG1
T1/ST2
1.1 ± 0.3
0.5 ± 0.1*
ILC2 per 1000 islets
F
p=0.057
Insulin (ng/ml)
2.8 mM
16.7 mM
IgG
αCD90.2
G
Rag2-/-γc-/-
p = 0.07
Glucose (mmol/L)
PBS + IL-33
ILC2 + IL-33
Time (min)
H
Insulin (ng/ml)
2.8 mM
16.7 mM
PBS + IL-33
ILC2 + IL-33
I
Insulin (ng/ml)
2.8 mM
16.7 mM
Medium
ILC2-CM

Figure 5

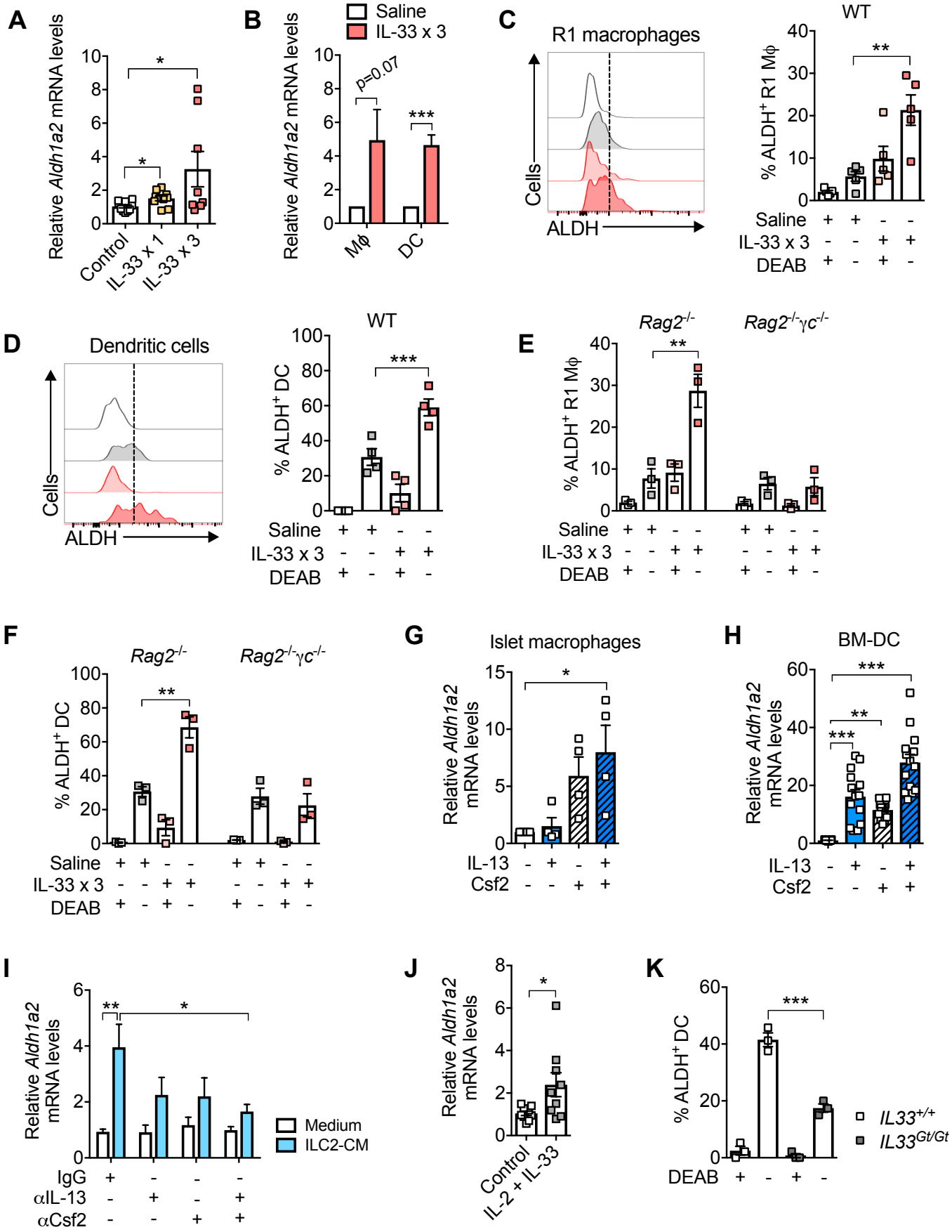
A
Relative Aldh1a2 mRNA levels
Control
IL-33 x 1
IL-33 x 3
B
Saline
IL-33 x 3
p=0.07
Mϕ
DC
C
R1 macrophages
Cells
ALDH
WT
% ALDH+ R1 Mϕ
Saline
IL-33 x 3
DEAB
D
Dendritic cells
% ALDH+ DC
E
Rag2-/-
Rag2-/-γc-/-
F
G
Islet macrophages
IL-13
Csf2
H
BM-DC
I
IgG
αIL-13
αCsf2
Medium
ILC2-CM
J
Control
IL-2 + IL-33
K
IL33+/+
IL33Gt/Gt

Figure 6

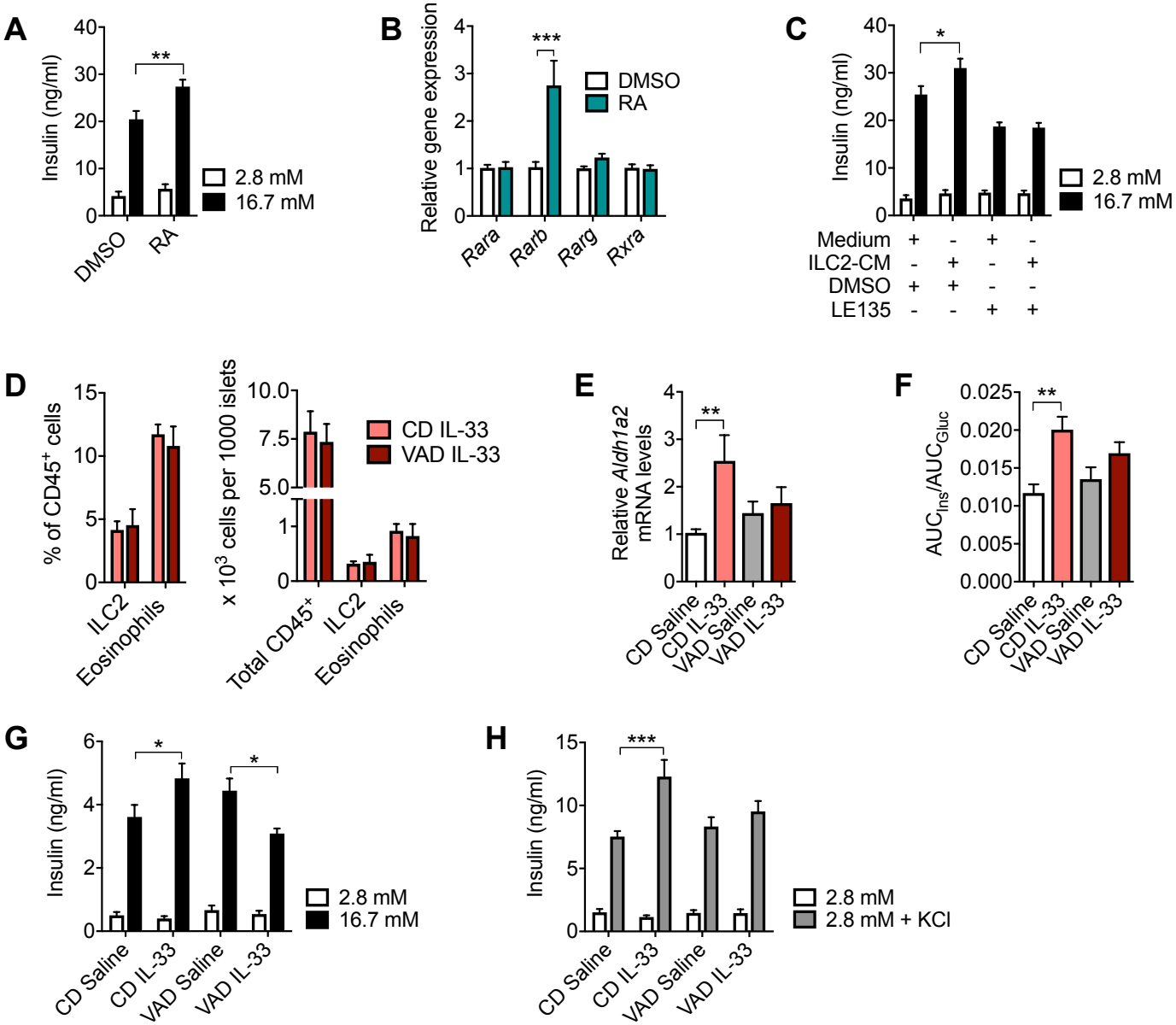
A
Insulin (ng/ml)
2.8 mM
16.7 mM
DMSO
RA
B
Relative gene expression
DMSO
RA
Rara
Rarb
Rarg
Rxra
C
Insulin (ng/ml)
2.8 mM
16.7 mM
Medium
ILC2-CM
DMSO
LE135
D
% of CD45+ cells
ILC2
Eosinophils
x 10^3 cells per 1000 islets
CD IL-33
VAD IL-33
Total CD45+
ILC2
Eosinophils
E
Relative Aldh1a2 mRNA levels
CD Saline
CD IL-33
VAD Saline
VAD IL-33
F
AUCIns/AUCGluc
CD Saline
CD IL-33
VAD Saline
VAD IL-33
G
Insulin (ng/ml)
2.8 mM
16.7 mM
CD Saline
CD IL-33
VAD Saline
VAD IL-33
H
Insulin (ng/ml)
2.8 mM
2.8 mM + KCl
CD Saline
CD IL-33
VAD Saline
VAD IL-33

Figure 7

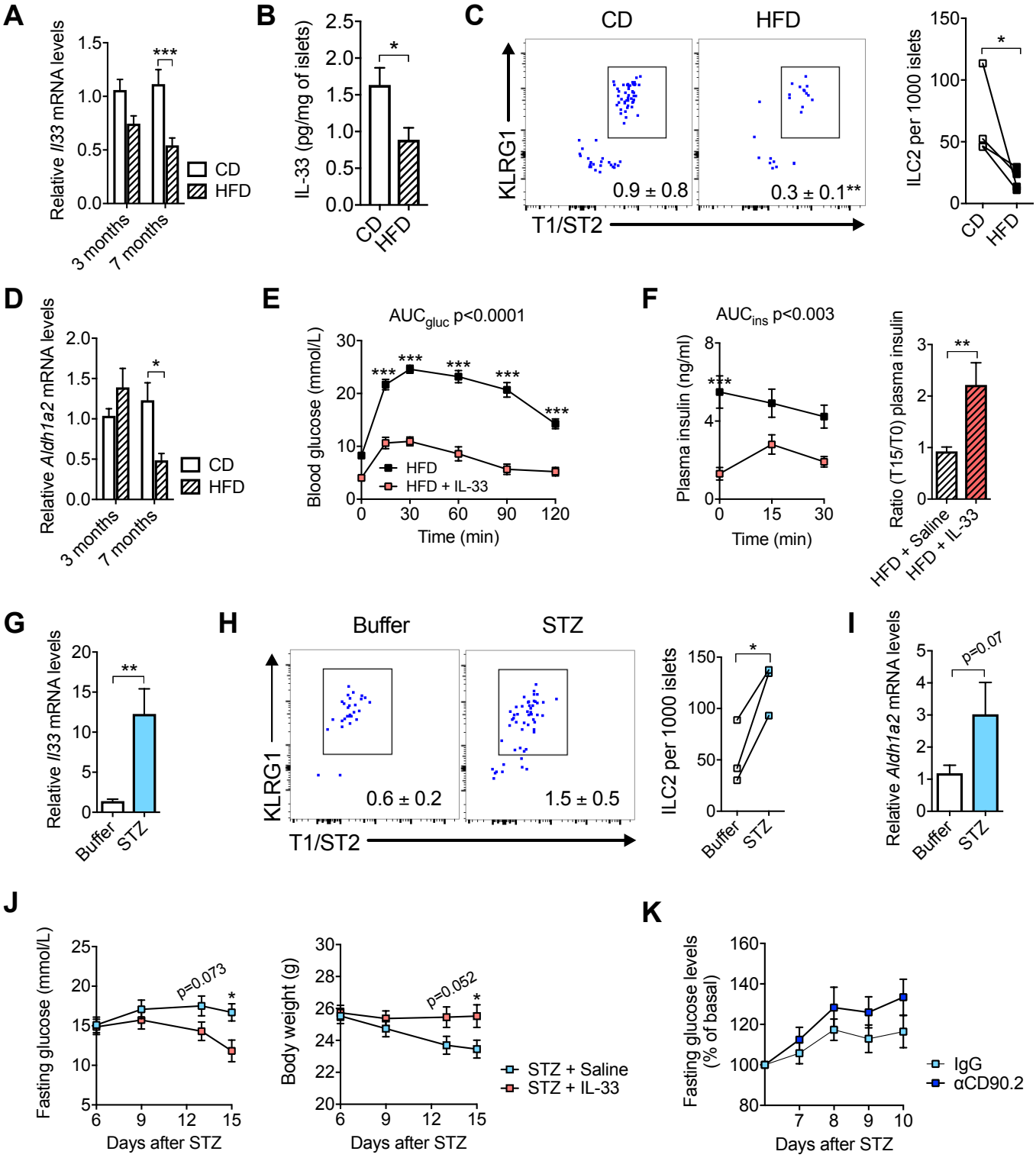
A
Relative Il33 mRNA levels
1.5
1.0
0.5
0.0
***
CD
HFD
3 months
7 months
B
IL-33 (pg/mg of islets)
2.5
2.0
1.5
1.0
0.5
0.0
*
CD
HFD
C
CD
HFD
KLRG1
T1/ST2
0.9 ± 0.8
0.3 ± 0.1**
ILC2 per 1000 islets
150
100
50
0
*
CD
HFD
D
Relative Aldh1a2 mRNA levels
2.0
1.5
1.0
0.5
0.0
*
CD
HFD
3 months
7 months
E
AUCgluc p<0.0001
Blood glucose (mmol/L)
30
20
10
0
***
HFD
HFD + IL-33
0
30
60
90
120
Time (min)
F
AUCins p<0.003
Plasma insulin (ng/ml)
8
4
0
***
0
15
30
Time (min)
Ratio (T15/T0) plasma insulin
3
2
1
0
**
HFD + Saline
HFD + IL-33
G
Relative Il33 mRNA levels
20
15
10
5
0
**
Buffer
STZ
H
Buffer
STZ
KLRG1
T1/ST2
0.6 ± 0.2
1.5 ± 0.5
ILC2 per 1000 islets
150
100
50
0
*
Buffer
STZ
I
Relative Aldh1a2 mRNA levels
5
4
3
2
1
0
p=0.07
Buffer
STZ
J
Fasting glucose (mmol/L)
25
20
15
10
5
p=0.073
*
6
9
12
15
Days after STZ
Body weight (g)
30
28
26
24
22
20
p=0.052
*
6
9
12
15
Days after STZ
STZ + Saline
STZ + IL-33
K
Fasting glucose levels (% of basal)
160
140
120
100
80
7
8
9
10
Days after STZ
IgG
αCD90.2